ANNUAL REVIEWS

Annual Review of Biochemistry

Eukaryotic Ribosome Assembly

Jochen Baßler and Ed Hurt

Biochemistry Center, University of Heidelberg, 69120 Heidelberg, Germany;
email: jochen.bassler@bzh.uni-heidelberg.de, ed.hurt@bzh.uni-heidelberg.de

Annu. Rev. Biochem. 2019. 88:281–306

First published as a Review in Advance on December 19, 2018

The *Annual Review of Biochemistry* is online at biochem.annualreviews.org

https://doi.org/10.1146/annurev-biochem-013118-110817

Keywords

ribosome assembly, ribosome biogenesis, rRNA processing, cryo–electron microscopy, in vitro reconstitution, nucleolar stress response, cancer target, ribosomopathies

Abstract

Ribosomes, which synthesize the proteins of a cell, comprise ribosomal RNA and ribosomal proteins, which coassemble hierarchically during a process termed ribosome biogenesis. Historically, biochemical and molecular biology approaches have revealed how preribosomal particles form and mature in consecutive steps, starting in the nucleolus and terminating after nuclear export into the cytoplasm. However, only recently, due to the revolution in cryo–electron microscopy, could pseudoatomic structures of different preribosomal particles be obtained. Together with in vitro maturation assays, these findings shed light on how nascent ribosomes progress stepwise along a dynamic biogenesis pathway. Preribosomes assemble gradually, chaperoned by a myriad of assembly factors and small nucleolar RNAs, before they reach maturity and enter translation. This information will lead to a better understanding of how ribosome synthesis is linked to other cellular pathways in humans and how it can cause diseases, including cancer, if disturbed.

Contents

INTRODUCTION

Ribosomes are the molecular machines that produce all cellular proteins during a complex and highly regulated biochemical process termed translation. The eukaryotic 80S ribosome consists of a small 40S subunit and a large 60S subunit. The 40S subunit comprises the 18S ribosomal RNA (rRNA) and 33 different ribosomal proteins [r-proteins; those of the small subunit (SSU) are designated Rps], whereas the 60S subunit consists of 25S, 5.8S, and 5S rRNA together with 47 r-proteins [Rpl in the large subunit (LSU)] (for a detailed survey of ribosome composition, structure, and nomenclature, see References 1, 2).

During the complicated biogenesis of eukaryotic ribosomes, the rRNA is folded, modified, processed, and assembled with r-proteins to form the two ribosomal subunits (**Figure 1**). This process takes place largely in a specialized nuclear compartment, the nucleolus, and can be divided into five major activities: synthesis of the preribosomal RNA (pre-rRNA) and r-proteins, base modification of the pre-rRNA, folding of the pre-rRNA, assembly of the pre-rRNA with the r-proteins, and endo- and exonucleolytic processing of the pre-rRNA to remove external and internal transcribed spacer rRNAs (5′-ETS, ITS1, ITS2, 3′-ETS) (**Supplemental Figure 1*a***). In eukaryotes, this process is mediated by approximately 200 different biogenesis factors [also known as ribosome assembly factors (AFs)] and approximately 80 small nucleolar RNAs (snoRNAs). Most of these assembly and processing steps are tightly coupled and occur within preribosomal particles that travel, as folding and maturation progresses, from the nucleolus, through the nucleoplasm, and across nuclear pore complexes (NPCs) into the cytoplasm, where they ultimately mature into translation-competent ribosomal subunits (**Figure 1**). Ribosome assembly is the most energy-consuming process in a growing cell, requiring extensive regulation and coordination with other cellular pathways. Perhaps, then, it is no surprise that a growing number of diseases (termed ribosomopathies) are associated with defects in ribosome synthesis. Moreover, strong upregulation of ribosome assembly is an important molecular alteration of rapidly dividing cancer cells, owing to the high demand for ribosomes. All these findings make the entire ribosome synthesis machinery an attractive target for the treatment of cancer.

Supplemental Material >

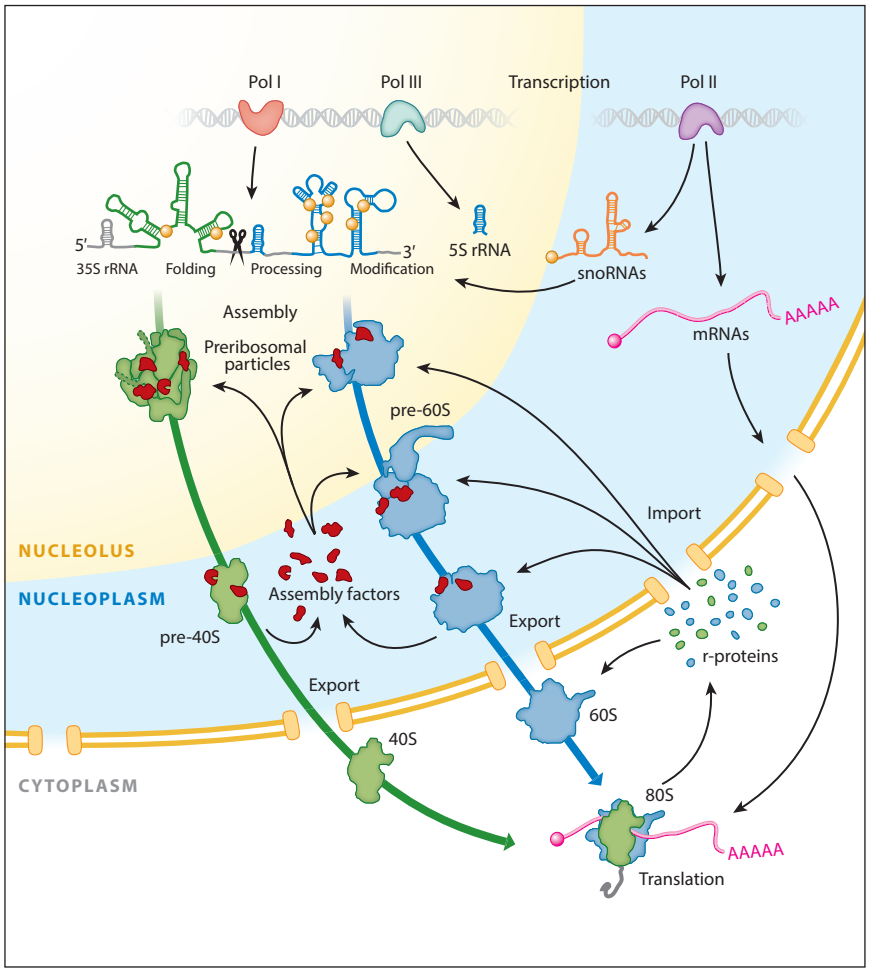

Figure 1

Overview of the eukaryotic ribosome assembly pathway. Ribosome assembly requires all three RNA polymerases: Pol I synthesizing the 35S rRNA precursor, Pol III synthesizing the 5S rRNA, and Pol II synthesizing snoRNAs and mRNAs, which also encode the ribosomal proteins (r-proteins). During transcription, the pre-rRNA is folded, nucleolytically processed, and modified (e.g., methylated or pseudouridinylated). Already at this early stage, ribosome assembly factors and r-proteins assemble with the nascent pre-rRNA to form preribosomal particles, which subsequently go through further maturation steps, thereby moving from the nucleolus and through the nucleoplasm into the cytoplasm, where mature 60S and 40S subunits join to form the 80S ribosomes, which translate the mRNAs into proteins. Abbreviations: mRNA, messenger RNA; pre-rRNA, preribosomal RNA; rRNA, ribosomal RNA; snoRNA, small nucleolar RNA.

In this review, we first provide an overview of the ribosome assembly path by charting the history that gave us the key discoveries and then highlight recent breakthroughs in the structural analysis of preribosomal particles. In addition, we describe how in vitro assays that reconstitute distinct preribosome maturation steps give unprecedented mechanistic insight when combined with structural findings. Finally, we refer to the importance of an intact ribosome assembly pathway in human cells for the sensitive balance between cell proliferation, cell cycle arrest, and apoptosis in health and disease conditions.

TIMELINE OF RIBOSOME BIOGENESIS RESEARCH

Identification of the rRNA Processing and Ribosome Assembly Pathways

The analysis of ribosome biogenesis has a long history. Fifty years ago, it was discovered that the two eukaryotic ribosomal subunits are assembled in the nucleolus from a common "giant" precursor rRNA. Pioneering insight came from radioactive pulse-labeling of RNA in mammalian cells, which revealed that initially this large ~45S rRNA precursor is cotranscriptionally modified and processed into 18S, 5.8S, and 28S rRNA in different subcellular compartments (3, 4). Sucrose gradient centrifugation studies of pulse-labeled RNA demonstrated the existence of preribosomal particles (termed 90S, 66S, and 43S) that contained these various radioactive pre-rRNA intermediates (5, 6). Notably, the 90S and 66S preribosomal particles had a higher protein to RNA ratio than mature subunits, which led to the postulate that these particles contain additional proteins besides the r-proteins (7). At that time, the use of an electron microscopy (EM) technique termed Miller spreads made nascent pre-rRNA transcripts visible, giving a first structural glimpse into the earliest ribosome assembly intermediates (8). Typically, Miller spreads revealed that several RNA polymerase I enzymes sequentially synthesize pre-rRNA along a single rDNA repeat in a Christmas-tree like pattern. Besides being the location for pre-rRNA transcription, the nucleolus also functions as a factory that houses the assembly line for the production of ribosomal precursor particles from r-proteins, which are made in the cytoplasm and imported into the nucleus, and the nascent rRNA. To fulfill this role, the nucleolus is highly organized into distinct subcompartments, which were initially identified by EM and immunolabeling of nucleolar proteins (9–11). The so-called fibrillar centers harbor the rDNA genes and polymerase I, and hence they are believed to be the site of rRNA transcription. The fibrillar centers are surrounded by the dense fibrillar compartment, where the nascent rRNA associates with both ribosomal and AFs. Finally, the granular compartment receives and further processes these preribosomal particles. Cell fractions analyzed for the different pre-rRNA processing intermediates suggested that processing of the large ~45S pre-rRNA leading to mature 28S and 5.8S rRNA takes place mainly in the nucleolus, but that final 18S rRNA processing occurs in the cytoplasm (12).

In later experiments, the use of the yeast *Saccharomyces cerevisiae* allowed the combination of genetic manipulation with pulse-chase labeling and biochemical assays to further dissect the eukaryotic ribosome assembly pathway. Similar to human cells, 90S, 66S, and 43S preribosomal particles were found in this fungus, demonstrating that ribosome assembly is conserved from yeast to humans (7, 13). However, despite progress in identifying most of the r-proteins and being able to describe the course of pre-rRNA transcription, modification, and processing (reviewed in References 14, 15), the drivers of ribosome assembly remained unknown. This changed when the *trans*-acting factors were discovered on the basis of yeast genetic screens or raising antibodies against nucleolar proteins (reviewed in References 16, 17). Initially, these factors were named Drs (deficiency of ribosomal subunits; e.g., Drs1), Nop (nucleolar proteins; e.g., Nop1, Nop58), Mak (maintenance of killer plasmid; e.g., Mak21), Rrp (ribosomal RNA processing; e.g., Rrp1), Kre (killer resistance; e.g., Kre33), Ecm (extracellular matrix; e.g., Ecm16), or Spb (suppressor of Pab; e.g., Spb4), with the number behind the gene name either indicating the molecular weight (kDa) or reflecting the chronological order of discovery.

Besides AFs, groups of snoRNAs, which clearly differ from the spliceosomal small nuclear RNAs, were found to play a key role in early ribosome assembly (18). In particular, the U3 snoRNA identified in the 1970s (19, 20) has been recognized as a key driver of pre-rRNA processing reactions and hence has garnered much interest. Pioneering work on the U3 snoRNP (small nucleolar ribonucleoprotein particle) composition and assembly came from the Lührmann laboratory (21), whereas the laboratories of Tollervey, Steitz, and Pederson demonstrated U3 hybridization to 18S

pre-rRNA (20, 22, 23). Additionally, snoRNAs such as U14 and snR30 were shown to be required for endonucleolytic cleavage of the pre-rRNA at distinct sites, known as A_0, A_1, and A_2 in yeast (24–26) (**Supplemental Figure 1*a***). Thus, pre-rRNA processing resembles pre-mRNA (messenger RNA) splicing, except that cleaved rRNA fragments remain unjoined and are trimmed by exo- and endonucleolytic enzymes to yield the mature rRNA species (27–29).

Supplemental Material >

Subsequently, approximately 80 snoRNAs were identified, mostly by bioinformatic searches, and grouped into two major classes: (*a*) ~45 C/D box snoRNAs, which include U3, U14, and snR190, commonly immunoprecipitated by antifibrillarin (Nop1) antibodies or antibodies against the trimethylguanosine 5′ cap structure; and (*b*) ~30 H/ACA box snoRNAs, which differ in secondary structure and associated proteins (27, 30, 31). Importantly, most of the C/D box snoRNPs (except U3, U14, and snR30) were recognized as having a role in 2′-*O*-ribose methylation at numerous rRNA sites by the snoRNP-associated fibrillarin/Nop1. In contrast, H/ACA box members are involved in snoRNA-guided pre-rRNA pseudouridinylation, catalyzed by the pseudouridine synthase Cbf5 (18, 27). As this mechanism requires a (locally) unfolded rRNA for the snoRNA–pre-rRNA hybridization, it is widely accepted that these modifications occur largely during transcription and initial folding of the pre-rRNA. Surprisingly, these snoRNAs turned out to be nonessential for yeast cell growth, even if several of them were knocked out. However, a few snoRNPs, which are essential for ribosome assembly, do not modify pre-rRNA, but keep the pre-rRNA unfolded or immature at specific sites, and in addition give structural support for the assembly and maturation processes of different preribosomal particles (e.g., U3 snoRNP; see the section titled Atomic Structure of the 90S Preribosome). Additionally, a few base modifications occur at the later stages of preribosome assembly if the particles have already reached a significant maturation stage. In these cases, specific methyltransferases (32–34) or acetylases (35) act without the support of guide snoRNAs. Astonishingly, the result of all these modifications was recently visualized by cryo–electron microscopy (cryo-EM), showing 130 individual rRNA methylations and pseudouridinylations in the 3D structure of the human 80S ribosome (36).

Besides the snoRNPs, 19 helicases have been implicated in yeast to participate in ribosome assembly, in particular in the earlier steps, but their precise roles in most cases remain unclear (37). This is partly due to their rather transient association with preribosomal particles. Hence, it is commonly believed that these helicases function to dismantle snoRNAs from the pre-rRNA or in remodeling the pre-rRNA to promote correct folding and/or processing.

Nuclear Export of Preribosomal Particles

At the beginning of the new millennium, the mechanism of nuclear export of ribosomal subunits was addressed by performing visual screens that detected mislocalized preribosomal subunits in mutant yeast cells. These assays were based on GFP-tagged r-proteins, which served as reporters to reveal the nuclear accumulation of preribosomal particles under mutant conditions (38), or they used in situ hybridization to detect mislocalized pre-rRNA intermediates (39). Together, these screens revealed that nucleoporins, the Ran-GTPase system, and its cooperating nuclear export receptors (exportins, karyopherins) are involved in both 60S and 40S subunit export but that nuclear import factors (importins) are also required to supply the nucleus with r-proteins and biogenesis factors. In addition, dedicated chaperones assist in the nuclear import and subsequent loading of several r-proteins onto these early preribosomal particles, thereby contributing to their hierarchical incorporation (for recent reviews, see References 40, 41). To drive nuclear export, a nuclear export sequence (NES) containing adaptor protein, such as Nmd3, recruits the Crm1/Xpo1 export receptor to the pre-60S subunit to facilitate its nuclear export (39, 42–45). However, additional noncanonical export factors were detected on the nascent 60S

subunit, leading to the view that the relatively large preribosomal export substrates require more than one transport factor for efficient nuclear exit (for overview, see 46). Similarly, the pre-40S subunit is also exported in a RanGTP-dependent mechanism involving the Crm1/Xpo1 export receptor (46); this finding was supported by the identification of several NES-containing adaptor proteins specifically bound to the SSU (47–49). However, it remains unclear how export competence is gained during 40S biogenesis and how the multiple transport factors cooperate in SSU export.

Biochemical and First Structural Characterization of Preribosomal Particles

Initially, it was unclear whether preribosomal particles, which were thought to be rather labile and of low abundance, could be purified. However, in 2001 this assumption was disproven when the first preribosomal particles were biochemically isolated by the powerful tandem affinity purification method. This approach revealed the biochemical complexity of the ribosome assembly pathway, as many long-sought AFs were copurified and subsequently identified by mass spectrometry (50–53). Ordering these different preribosomal particles from early nucleolar to intermediate nucleoplasmic and late cytoplasmic particles finally established a first road map of ribosome biogenesis (reviewed in Reference 54) (**Figure 1**).

After the identification of 200 diverse AFs, the focus of research shifted toward clarifying the spatiotemporal order of the interactions between the nascent rRNA, AFs, and r-proteins. Soon it was recognized that different preribosomal particles carry specific modules (55–60) and different r-proteins (61, 62), which was also made possible with the development of further sophisticated assays, including stringent and large-scale affinity purifications (63), yeast two-hybrid screens (64–66), biochemical reconstitution (66–69), protein–RNA crosslinking experiments (CRAC) (70), and purification of epitope-tagged pre-rRNA truncation constructs and characterization of associated factors (71–73).

After these biochemical advances, interest grew in gaining insight into the structure of both ribosome biogenesis factors and complete preribosomal particles. Initially, negative-stain and simple cryo-EM revealed that preribosomal particles resemble mature subunits in some regions, whereas other structural features either were associated with AFs or contained extra RNA (e.g., 5′-ETS, ITS2) or unfolded rRNA (74–76). The next progression toward a deeper structural understanding happened when the density maps of preribosomal particles reached sub-nanomolar resolutions (approximately 8–16 Å) (77–79). In parallel, mature subunits were reconstituted with recombinant ribosome biogenesis factors and analyzed by cryo-EM, which also allowed visualization of predominant late AFs (80–84). Altogether, these cryo-EM maps revealed secondary structural elements of AFs, which made it possible to fit high-resolution X-ray structures or in silico molecular models of AFs (78–80, 85–88). This approach was reinforced by structural analysis on thermostable AFs from *Chaetomium thermophilum* (89, 90). However, further modeling and crystallization were hindered by the lack of tertiary structures in many conserved AFs, which instead are natively unfolded or contain long extensions and/or large internal loops. Nevertheless, X-ray crystallography might remain an important method to obtain high-resolution structures of delicate AFs that are only flexibly attached to preribosomal particles (91).

In 2014, cryo-EM underwent a tremendous technological revolution at a rapid pace, with advances in detector hardware and image-processing software that allowed the complex molecular structures of preribosomes to be solved at near-atomic resolution (reviewed in 92–95). This resolution revolution in cryo-EM enabled unprecedented insight into how pre-rRNA, r-proteins, snoRNAs, and the myriad of AFs are organized within preribosomal particles, which is the focus of the next section.

RIBOSOME ASSEMBLY PATHWAY IN HIGH STRUCTURAL RESOLUTION

Atomic Structure of the 90S Preribosome

Supplemental Material >

During the transcription of the 35S rRNA precursor, the first modules, UTP-A and UTP-B, are recruited to the growing 5′-ETS (**Figure 1**; **Supplemental Figure 1*a***), before further AFs associate in a hierarchical order with the growing pre-rRNA to form the first stable preribosomal intermediate, which is amenable to biochemical isolation. These particles are termed either the 90S preribosome (the historical name, which is used here) or the SSU processome (55, 56, 58). The cryo-EM structures of these 90S preribosomes, isolated from either *C. thermophilum* or yeast, were initially solved at 4.5- to 6.5-Å resolution, which was later refined to 3.2 Å, beyond the critical threshold of ~4 Å necessary to achieve pseudoatomic resolution (85, 86, 96–98) (**Figure 2**). This advance revealed how the nascent 18S pre-rRNA carrying the entire folded 5′-ETS (notably, the noncleaved A_1 site is clearly visible in these structures) and the early attached Rps proteins are embedded in a casting mold formed by ~60 biogenesis factors and the U3 snoRNP (**Figure 2*b***; **Supplemental Table 1**). This scaffold provides an encapsulated and protected environment for the subsequent processing and maturation steps (**Figure 2*b***). Compared with the mature 18S rRNA with its typical folded 5′, central, 3′ major, and 3′ minor subdomains (**Supplemental Figure 1*b***), only the 5′ domain is close to its mature conformation and accordingly carries its cognate r-proteins. However, the central domain is only partially visible, and little of the 3′ domain can be recognized in the 90S structure (**Figure 2*c***). Thus, it appears that folding of the nascent 18S rRNA progresses from the 5′ to the 3′ end but is locked at an intermediate stage that requires recruitment of further AFs and other suspected triggers (e.g., ATP or GTP to provide chemical energy) for the next maturation steps (**Figure 1**).

Notably, the 90S cryo-EM structures revealed how the folded 3′ part of the U3 snoRNA carries the C/D box core factors (Nop1, Nop56, Nop58, Snu13, Rrp9) and partly protrudes from the 90S particle, whereas the single-stranded 5′ half deeply penetrates the interior of the particle, hybridizing via conserved short nucleotide motifs to the nascent 18S rRNA and 5′-ETS (**Figure 2*d***). This latter finding enables the considerable amount of published genetic and biochemical data on this snoRNA to be interpreted in a structural context. In particular, U3 has been suggested to maintain specific regions of the 35S pre-rRNA in a premature stage, which is crucial for timely endonucleolytic processing at sites A_1 and A_2. This exact premature conformation was visualized by cryo-EM studies, which explained at the molecular level how the U3 snoRNA hinders formation of the central pseudoknot, a hallmark RNA structure and part of the decoding center in the mature 18S rRNA (**Figure 2*d***).

The 90S preribosome carries many more biogenesis factors, including the UTP-A, UTP-B, UTP-C, Mpp10–Imp3–Imp4, and Bms1–Rcl1 modules (**Figure 2**; **Supplemental Table 1**). It was interesting to see the GTPase Bms1 at high resolution in the 90S structure, as this energy-consuming enzyme is thought, upon GTP hydrolysis, to trigger conformational changes that eventually induce pre-rRNA processing coupled to the 90S > pre 40S progression. Consistent with this hypothesis, Bms1 is strategically located at the interface of the different pre-18S domains, with extensive contact to several other AFs that stabilize the transient structure of the 90S particle (**Figure 2*e***).

Approximately 18 of the ~60 AFs in the 90S particle are β-propeller proteins, which provide a scaffold for protein–protein interactions, as typically found in many other macromolecular assemblies [e.g., NPCs and COPI and COPII proteins of the vesicular transport machinery (99)] (**Figure 2*f***). In addition, several tryptophan–aspartic acid (WD) repeat proteins of the 90S preribosome bind directly to specific rRNA sites. Another prominent group of AFs present on the

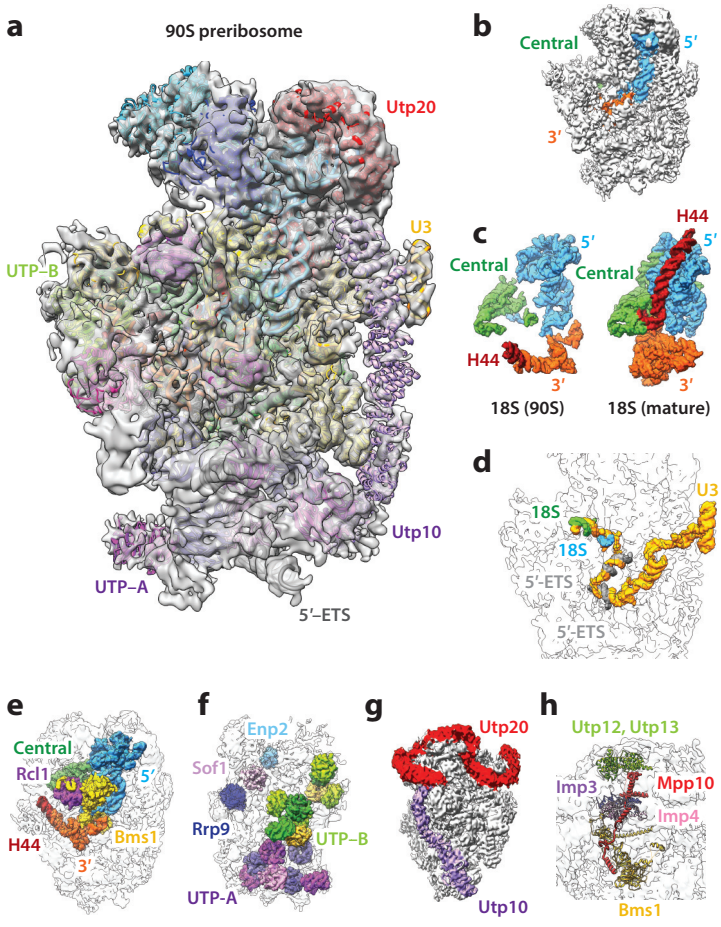

Figure 2

Cryo–electron microscopy (cryo-EM) structure of the 90S preribosomal particle isolated from *Chaetomium thermophilum*. (*a*) The cryo-EM structure of the 90S preribosome with rRNA, r-proteins, U3 snoRNA, and assembly factors shown in ribbon representation. (*b*) The 18S pre-rRNA (5′ domain shown in *light blue*, central domain in *green*, and 3′ domains in *orange* and *red*) is encapsulated by a scaffold of biogenesis factors (*gray*). (*c*) The conformation of the 18S rRNA domains inside the 90S particle is compared with the conformation of the mature 18S rRNA. (*d*) The U3 snoRNA (*yellow*) penetrates deeply into the 90S structure, where its 5′ single-stranded RNA sequence hybridizes to specific sites within the 5′-ETS (*light blue*) and 18S rRNA (*green*). (*e*) The Bms1 GTPase (*yellow*) and its cofactor Rcl1 (*purple*) are located centrally in the 90S particle, contacting all domains of the 18S pre-rRNA. (*f*) The 90S particle contains multiple β-propeller proteins, many of them organized within the UTP-A and UTP-B subcomplexes. (*g*) The β-solenoid protein Utp10 (*purple*) connects the 5′-ETS (*bottom*) with the nascent 5′ domain, which is organized by Utp20 (*red*). (*h*) The meandering Mpp10 protein (*red*) contacts multiple factors including Bms1 (*yellow*), the Brix factor Imp4 (*pink*), Imp3 (*purple*), and the Utp12–Utp13 interface (*green*). Figures were prepared in Chimera using EMD 8143 and Protein Data Bank structures 5oql and 5jpq.

90S particle are α-helical proteins. The large α-solenoid proteins Utp20 (~220 kDa) and Utp10 (~180 kDa) are intriguing, as they can reach distant areas on the 90S particle with their highly elongated α-solenoid structures. For example, Utp10 spans from the base of the 90S, where the 5′-ETS is embedded, to the top of the 90S (5′ domain), where it contacts Utp20, which itself

wraps around the head of the 90S particle (**Figure 2*g***). Such long-distance contacts might facilitate communication between different areas and/or contribute to sensing the overall conformation to coordinate subsequent maturation steps.

In contrast to AFs with a tertiary structure, some 90S biogenesis factors are partially or completely unfolded. These polypeptide chains are often found meandering across the surface or deeply penetrating the 90S core structure. One typical example is Mpp10, which upon winding through the 90S, gains contacts to Imp3, Imp4, Bms1, Utp12, Utp13 (UTP-B), and parts of the 18S rRNA via distinct motifs (**Figure 2*b***). Similarly, Nop14 makes contacts via its long N- and C-terminal extensions to Noc4, Emg1, and Rcl1. In this way, such sequence elements not only stabilize the 90S preribosome but also participate in long-distance interaction and/or conformational sensing.

The ultimate fate of the 90S preribosome is a transition stage, from which the pre-40S particle is released, leaving its covering scaffold mold behind. This step is tightly coordinated with the cleavage of the 35S precursor at sites A_1 and A_2, which is also the prelude for the 60S biogenesis pathway (see the section titled The Structure of the Late 40S Preribosome) (reviewed in 100, 101) (**Figure 1**; **Supplemental Figure 1*a***). Currently, the PIN domain protein Utp24 is a good candidate for being the endonuclease that catalyzes the coordinated A_1–A_2 site cleavages (102–104). However, the Karbstein laboratory has reported that Rcl1 is the long-sought A_1–A_2 site endonuclease (105). Interestingly, Utp24 is located close to site A_1 in the 90S particle but cannot fulfill its function because another AF, Sof1, masks the A_1 cleavage site. Thus, to reach a transition-competent stage, the 90S preribosome requires considerable conformational rearrangements and association of new AFs (e.g., helicases) or energy input.

Supplemental Material >

Several additional enzymes, for example the acetyltransferase Kre33 or the methyltransferases Nop1 and Emg1, are present on the 90S particle. Stably associated helicases are absent, although some have been strongly implicated in 90S assembly and maturation. It is conceivable that the 90S > pre-40S transition is stimulated by the Dhr1/Ecm16 helicase, for which evidence has been presented that it breaks the base pairing between the U3 snoRNA and the pre-rRNA (106, 107). However, the details of this process remain unknown, and it will be challenging to develop in vitro assays for this maturation step. During the 90S > pre-40S transition step, the 5′-ETS particle seems to split off en bloc, carrying the 5′ ETS RNA together with UTP-A, UTP-B, U3 snoRNP, and a number of other biogenesis factors (85). Subsequent degradation of the 5′-ETS by the nuclear exosome might lead to its complete disassembly and recycling of biogenesis factors. Biochemical and structural characterization of additional 90S assembly and the 90S > 40S transition intermediate, awaiting their isolation and characterization, might fill gaps in the spatiotemporal assembly pathway.

The Structure of the Late 40S Preribosome

How pre-40S particles develop from the 90S preribosome is unclear at present, but the pre-40S particles that have been purified to date and analyzed by biochemical and structural methods exhibit a relatively simple AF composition (**Supplemental Table 1**) with a significantly matured 18S rRNA structure. The first cryo-EM map of a pre-40S particle revealed a nearly matured 5′ and central (platform) domain, whereas the 3′ major domain (head and beak regions) appeared immature, which was supported by biochemical data (76). In later studies, improved cryo-EM maps of pre-40S particles isolated from yeast and human cells demonstrated significant structural conservation of the positions of associated late AFs that occupy functionally important sites and block the interactions of the translation machinery (77, 79, 87). However, high-resolution structures could only be obtained after the aforementioned breakthrough in cryo-EM resolution, which

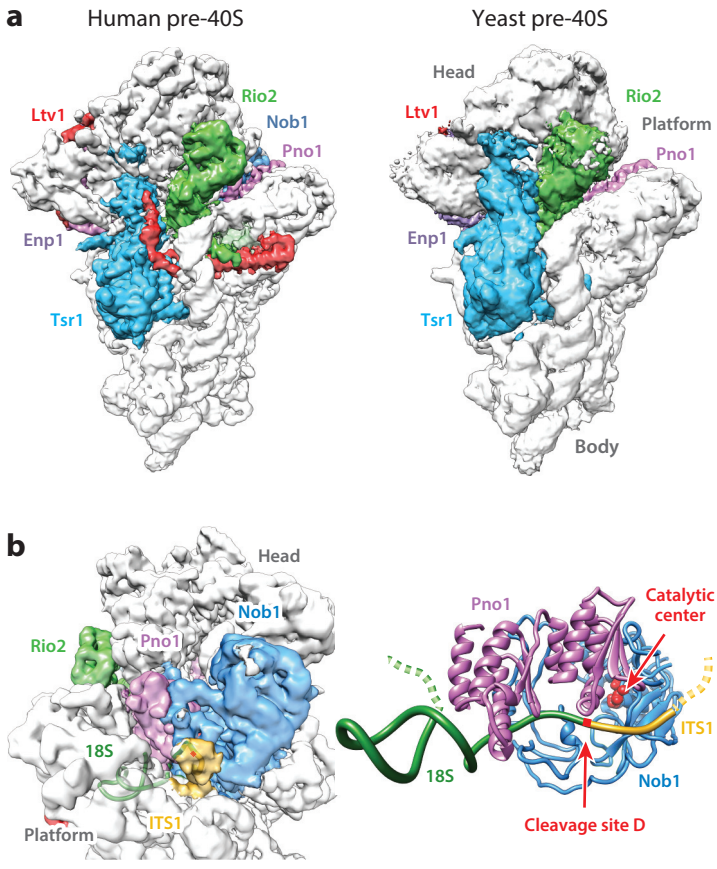

Figure 3

Evolutionary conservation of pre-40S particles from yeast to human. (*a*) Comparison of cryo-EM structures of pre-40S particles from human (*left*) and the yeast *Saccharomyces cerevisiae* (*right*). The subunit interface of the pre-40S particles with the characteristic head, platform, and body domains is shown, and the conserved pre-40S assembly factors are highlighted in the same colors. (*b*) The structure of the Nob1–Pno1/Dim2 dimer on the human pre-40S particle. The left panel depicts the EM volume of Pno1 (*light purple*) and Nob1 (*blue*) binding the neighboring rRNA sequences of the cleavage site D, between platform and head domain of the pre-40S particle. The right panel shows the derived pseudoatomic structure (ribbon model) of the Nob1–Pno1 heterodimer contacting the 18S and ITS1 rRNA at cleavage site D. Note that Pno1 masks cleavage site D, hindering the catalytic center of the Nob1 endonuclease to attack its substrate. The catalytic residues of the nucleolytic center of Nob1 (*filled red residues*) and the cleavage site D (*arrow*) are highlighted. Figures were prepared in Chimera using EMD 4337 (human), EMD 4214 (yeast), and PDB structure 6g18. Abbreviations: cryo-EM, cryo–electron microscopy; EM, electron microscopy; PDB, Protein Data Bank; rRNA, ribosomal RNA.

demonstrated a number of principles on how the yeast SSU assembly intermediate is organized at the molecular level and how it differs from mature 40S subunits (108, 109). Specifically, the major 40S subunit active sites such as the decoding center and mRNA binding groove are not formed, but the AFs Tsr1, Enp1, Rio2, and Pno1/Dim2 collectively control these immature sites, allowing coordinated and timely maturation of the 18S pre-rRNA (**Figure 3*a***). In the premature 3′ major domain (head and beak), Enp1 and Ltv1 occupy the binding site of ribosomal eS10 but are released in subsequent steps upon phosphorylation/dephosphorylation of Ltv1 and Enp1, involving

the Hrr25 protein kinase (76, 110, 111). Connected to Enp1-Ltv1 release is the recruitment of eS31 and relocation of the uS3 C-terminal domain, thus stabilizing the interface between the 40S body and head (108).

Moreover, the mechanism of the timely 20S pre-rRNA cleavage by the endonuclease Nob1 could be deduced from the cryo-EM structures. The RNA-binding protein Pno1 masks the cleavage site at the 3′ end of the mature 18S rRNA, suggesting the Nob1 endonuclease requires structural rearrangement to reach its substrate RNA. This might be achieved by coupling Nob1-dependent 20S > 18S processing to a quality control step, in which the pre-40S particle is checked for its proper interaction with the mature 60S subunit (112–117). Such a translation-like cycle was suggested to trigger final processing at site D and release of the remaining biogenesis factors. Coupling the formation of such an 80S-like particle with final 18S rRNA maturation might be a way of guaranteeing that only correctly assembled 40S subunits enter translation.

Recently, cryo-EM structures of different late human pre-40S particles were reported by the Beckmann laboratory, ranging from nuclear to late cytoplasmic states (118). The structure of one earlier intermediate revealed the position of the biogenesis factor Rrp12 and the two methyltransferases Bud23 and Trm112 at the 40S head. A later cytoplasmatic pre-40S particle is highly similar to the yeast pre-40S subunit, with conserved AFs at identical positions (**Figure 3*a***). Additionally, the associated human endonuclease Nob1 was visualized in high resolution, indicating precisely how Pno1 masks the Nob1 cleavage site at the 3′ end in the 18S rRNA (**Figure 3*b***). Thus, amazingly, both the pre-40S structure and the final pre-18S rRNA processing mechanism are extremely conserved over one billion years of evolution.

High-Resolution Structures of the Early Nucleolar Pre-60S Particles Reveal Sequential rRNA Domain Folding

The initiation of the 60S assembly pathway in yeast is initiated by cotranscriptional A_2 cleavage within the 35S pre-rRNA, which generates a 5′ fragment, the 20S pre-rRNA remaining with the pre-40S particles (see the section titled Atomic Structure of the 90S Preribosome) and a 3′ fragment termed 27SA pre-rRNA (**Supplemental Figure 1*a***), which is the RNA precursor that enters the 60S biogenesis pathway. Currently, it is not clear how the initial steps in pre-60S assembly occur, but the early 27SA > 27SB rRNA processing is perhaps coupled with rRNA folding in the developing pre-60S particles. Only at significantly later stages is the ITS2 removed by a complicated processing reaction (see the next section). It is also currently not clear exactly when and how the 5S RNP (5S rRNA, uL18/Rpl5, uL5/Rpl11) is incorporated into these earliest pre-60S particles, but this incorporation happens in a twisted 5S RNP conformation and hence requires a conformational rotation by 180°, again occurring later in the 60S maturation pathway (88, 89). This step is coupled with formation of the peptidyl transferase center (PTC) and checked for correct occurrence through removal of Rsa4 by the huge Rea1 AAA-ATPase and GTP-hydrolysis-dependent Nog2/Nug2 dissociation (90, 119). Only if these checkpoints are passed can the recruitment of nuclear export factors to the pre-60S particle and nuclear exit occur (119). However, not all domains of the maturing pre-60S particle are coupled to a nucleus-controlled surveillance system, as pre-60S particles in mutant cells that did not correctly remove the ITS2 pre-rRNA and its associated factors can escape into the cytoplasm and even enter translation (120–122).

Supplemental Material >

To date, most of the obtained cryo-EM–based structural snapshots of nascent preribosomes are derived from the pre-60S assembly branch. These images gave intriguing insights into the structural maturation of the LSU: (*a*) the organization of the ITS2 rRNA with associated biogenesis factors (also known as the foot structure) (88); (*b*) the attachment of the 5S RNP in rotated intermediate arrangement (88, 89); (*c*) the successive occupancy of the peptide exit tunnel by

different biogenesis factors (84, 88); (*d*) the binding of biogenesis factors at the nascent PTC (90, 123), which serve as sensors for quality control (119); (*e*) the recruitment of nuclear export factors (82, 124); and (*f*) the release of the remaining biogenesis factors into the cytoplasm (83, 125). The structural details and implications from these intermediate nucleoplasmic and late cytoplasmic preribosomes have been recently reviewed and discussed in detail (93) and hence are not further outlined in this review. Instead, we focus on the recent high-resolution cryo-EM structures of the nucleolar pre-60S particles, which revealed the early pre-rRNA folding events and assembly with biogenesis factors and Rpl proteins.

As recently as the end of 2017, three laboratories presented high-resolution cryo-EM structures of nucleolar pre-60S particles, which revealed the folding mechanism of its pre-rRNA (126–128). Despite the fact that these particles contain the complete 27SB rRNA, not all of the known rRNA domains from I to IV were visible in these structures (**Figure 4*a–d***). The 5S rRNA, with its specific proteins uL18/Rlp5 and uL5/Rpl11, although recruited, was also not discernible in these particles,

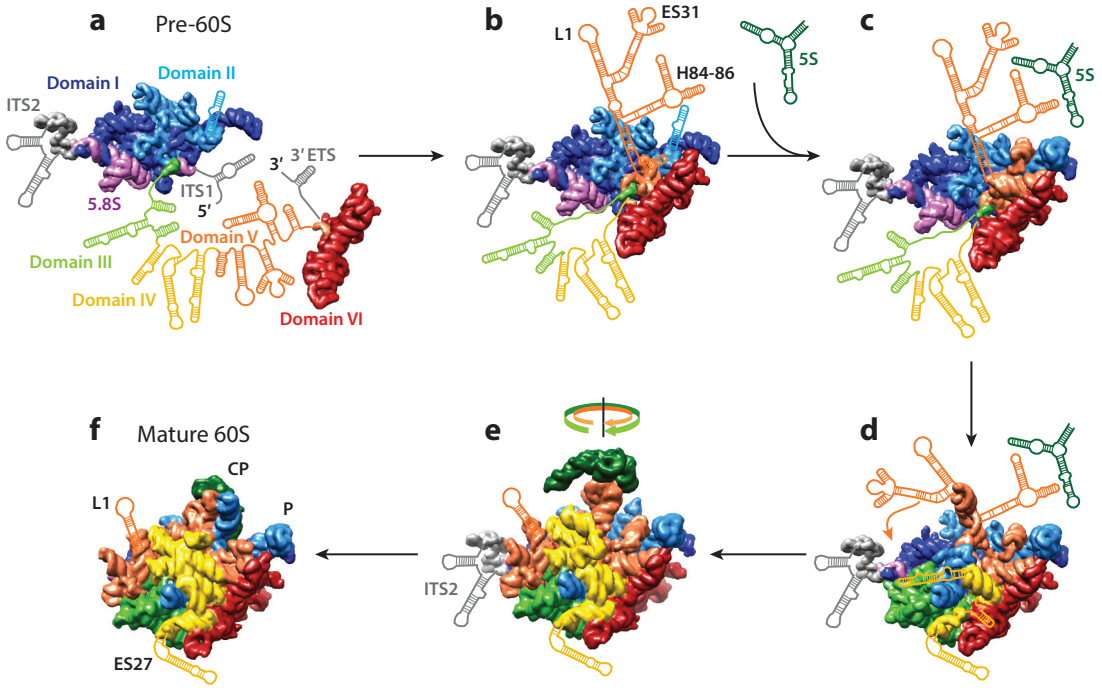

Figure 4

Folding and maturation of the 5.8S and 25S rRNA within the early nucleolar pre-60S particles. (*a*) The first rRNA precursor of the large subunit ($27SA_2$) contains ITS1, ITS2, domain I–IV, and 3′-ETS sequences (see also **Supplemental Figure 1**), for which structural information is not available. (*b*) Removal of ITS1 and 3′-ETS leads to 27SB pre-rRNA with assembled domains I, II, and VI, but domains III, IV, and V remain unstructured and are only schematically indicated. After stable incorporation of domain VI into the particle, part of (*c*) domain V and (*d*) domain III also become incorporated. The 5S RNP is also recruited at these stages. (*d–e*) At the next step, a major relocation of domain V occurs to bring the L1 stalk toward its mature position, which is stabilized by subsequent assembly of domain IV. (*e*) Subsequently, parts of domain V with attached 5S RNA twist by approximately 180° to form the mature central protuberance (CP), and ITS2 is removed to generate 5.8S and 25S rRNA (see **Figure 5** for details). (*f*) Final rearrangements include domains IV and V to form the active sites of the large subunit (A, P, and E tRNA binding sites), which is coupled to nuclear export. The rRNA was taken from PDB structures (*b*) 6em4, (*c*) 6em1, (*d*) 6em5, (*e*) 3jct, and (*f*) 4v88. An animation of the maturation process is presented in **Supplemental Video 1**. Abbreviations: ETS, external transcribed spacer; ITS, internal transcribed spacer; PDB, Protein Data Bank; rRNA, ribosomal RNA; tRNA, transfer RNA.

Supplemental Material >

suggesting that the 5S RNP is peripherally and/or flexibly attached, requiring further integration to reach the conformation typically seen in later pre-60S particles.

Initially, it was speculated that the 60S subunit assembles from the center to the periphery, around the most evolutionarily conserved part, the PTC. However, sorting the various nucleolar pre-60S particles according to the stably assembled rRNA domains (126–128) revealed a different mechanism (**Figure 4**). Presumably, the first rRNA domains, including 5.8S, ITS2, and domains I and II, fold and assemble into an initial rigid core particle, forming an exoskeleton for further assembly (**Figure 4*a***; **Supplemental Figure 1*c***). In this model, the ITS2 RNA and its associated biogenesis factors (Nsa3, Nop7, Erb1, Rlp7, Nop15) play an essential role, perhaps by facilitating the hybridization between 5.8S and domain I of the 25S rRNA (**Figure 5*b***). This model is supported by genetic findings that ITS2-processing mutants consistently impair early pre-rRNA processing (129–132). Thus, ITS2 could be a long-lasting structural element that is exploited as a scaffold for several 60S assembly steps, similar to what has been proposed for the 5′-ETS in the early 18S rRNA folding pathway (see the section titled Atomic Structure of the 90S Preribosome).

Supplemental Material >

Next, domain VI, which corresponds to the 3′ end of the 25S rRNA, is stably incorporated into the core particle, leading to ring closure of the rRNA but leaving domains III–V flexible (126–128) (**Figure 4*b***). Then, the remaining domains III–V are sequentially assembled around the later-developing exit tunnel, leaving the PTC in an immature conformation even when the particle exits the nucleolus. This sequence is in contrast to the 40S biogenesis pathway, where the rRNA folding follows a clear order from the 5′ to 3′ end of the 18S rRNA. Remarkably, a prerequisite for the formation of these ring-like 60S intermediates is the removal of ITS1 and the 3′-ETS (**Figure 4*a***; **Supplemental Figure 1*a***), as these sequences sterically hinder the association of the rRNA domain VI. Finally, the ring-like intermediate that covers both the 5′ and 3′ terminus of the rRNA can protect the rRNA against degradation but still might enable RNA modifications at flexible/exposed areas. Moreover, fixation of the 5′ and 3′ ends might facilitate the subsequent assembly of the flexible neighboring domains by acting as a scaffold. Domain V especially benefits from the prior assembly of the other rRNA domains, as its complicated folded rRNA makes contact with all other domains including the 5S rRNA (**Figure 4*f***) and has to pass through at least three different major conformations (**Figure 4*c,e,f***).

The early nucleolar pre-60S particles contain approximately 30 AFs and 30 r-proteins (**Supplemental Table 2**). Similar to the 90S particle, most of them seem to be important for structural stabilization. A few of these AFs also have enzymatic activity, which could drive key steps during the 60S assembly pathway. Among these catalytic factors are Nop2 and Spb1, which are important for non-snoRNP-dependent RNA methylation, whereas the substrate and function of the Has1 helicase remain elusive. Also, the (regulatory) functions of the GTPases Nog1 and Nug1, which might be particularly important for their release at later nuclear pre-60S particles, are not yet evident from their position in the structure. Interestingly, members of the Brix protein family that interact in a common manner with specific partner proteins (66, 133–135) seem to directly support rRNA folding by connecting different rRNA domains. Examples include the Ssf1–Rrp15 dimer, which bridges the rRNA domains III and VI; the Brx1–Ebp2 complex, which binds at the junction between domains I and II; and the Rpf1–Mak16 pair, which is in contact with the 5.8S rRNA and domains I, II, and VI. This model is reminiscent of how another Brix pair, Rpf2–Rrs1, interacts with the 5S rRNA and domain V in the successive Nog2 pre-60S particle (88) and how the Imp4–Mpp10 Brix complex connects the 5′-ETS and the nascent 3′ domain within the 90S particle (see the section titled Atomic Structure of the 90S Preribosome).

Many other structural components found on the Nsa1-purified pre-60S particle are found in groups or modules, such as the following: Nsa1–Rpf1–Mak16–Rrp1, which stabilizes the solvent-exposed surface; Rlp24–Nog1–Mrt4–Mak16–Tif6–Nsa2, which binds predominantly to domain

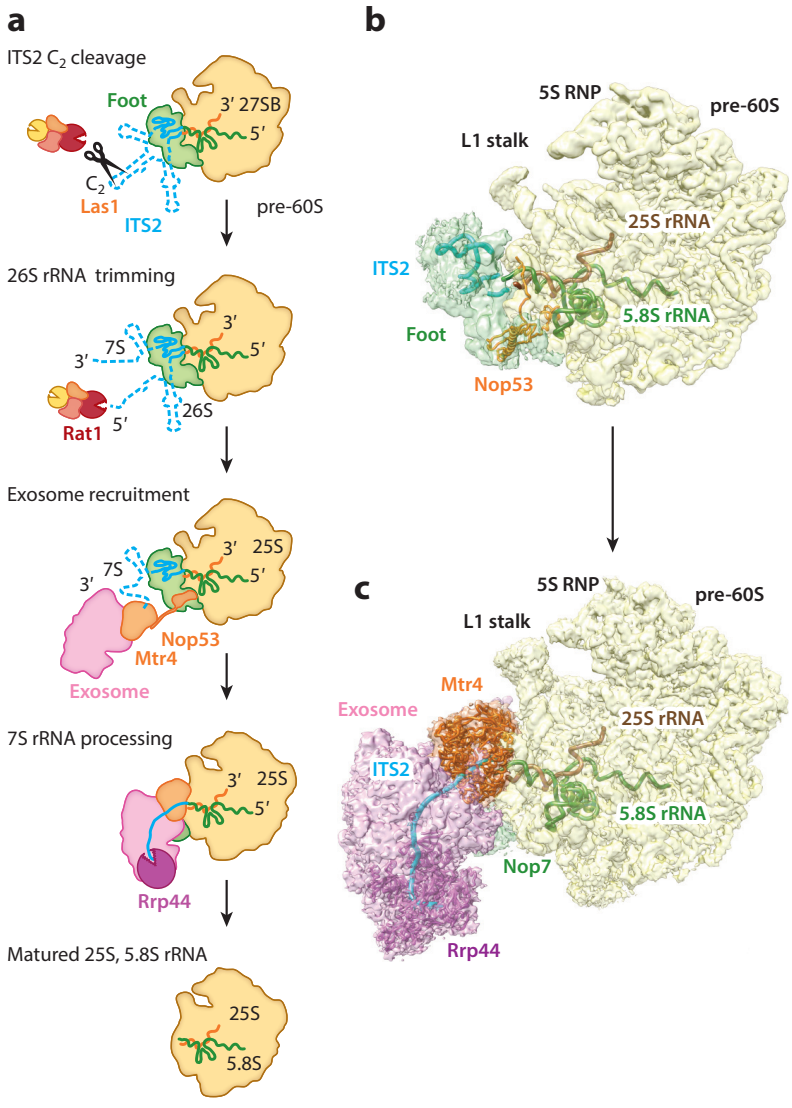

Figure 5

Removal of ITS2 from the pre-60S particle by the successive and coordinated action of different RNA processing enzymes. (*a*) Cartoon representation showing intermediates during ITS2 (*light blue*) removal. The endonuclease Las1 cleaves the ITS2 at site C_2, which generates 7S rRNA and 26S rRNA from the 27SB precursor rRNA. The resulting accessible ends are degraded by exonucleases. First, the 5′ end of 26S rRNA is trimmed by the Rat1 (26S > 25S′). The 7S is degraded by the nuclear RNA exosome, which is recruited to the pre-60S substrate particle via an interaction between pre-60S factor Nop53 (pre-60S) and the exosome cofactor Mtr4. It is predicted that the RNA helicase Mtr4 (*orange*) unwinds and channels the 3′ end of the 7S rRNA (*light blue*) into the exosome (*pink*), which could also displace most of the assembly factors of the foot structure. The structure of (*b*) the ITS2-containing pre-60S particle is compared with the structure of (*c*) the pre-60S intermediated with attached exosome. Figures were prepared in Chimera using EMD 6615, 4301, and 4302 and PDB structures 3jct, 6fsz, and 6ft6. Abbreviations: ITS, internal transcribed spacer; PDB, Protein Data Bank; rRNA, ribosomal RNA.

VI and V; and Nsa3–Nop15–Rlp3–Nop7–Erb1–Ytm1, which organizes ITS2 to form the foot structure. Similar to several 90S AFs, the AF Erb1 has a long N-terminal extension, which meanders over the pre-60S surface contacting many distant factors, including the Brx1–Ebp2 dimer, the Has1 helicase, Nop16, and the foot factor Nop7 (126–128). Moreover, Erb1 stably interacts via its β-propeller domain with Ytm1, which is a substrate of the Rea1 ATPase (136). At a certain step, Rea1 creates a mechanochemical force to remove Ytm1 and the deep-rooted Erb1. Notably, the other modules also contain targets (Nsa1, Rlp24) for active release by AAA-ATPases such as Rix7 and Drg1 (137, 138) and in this way act as further triggers for progression in pre-60S maturation. When all of these studies are combined, state-of-the-art cryo-EM provides near-atomic structural information about a complicated rRNA folding pathway in a movie-like fashion. Dozens of early AFs modify, chaperone, and stabilize immature rRNA conformations to allow a coordinated and strictly sequential ribosome assembly pathway.

In Vitro Assays Combined with Structural Studies Reveal the Mechanisms of Ribosome Assembly

A landmark breakthrough in the field of prokaryotic ribosome biogenesis was the in vitro reconstitution of the prokaryotic ribosomal subunits from purified molecular components (139). In contrast, in vitro assembly of eukaryotic ribosomal subunits is inconceivable considering the complexity of the rRNA processing and maturation pathway. However, in vitro assays were developed to monitor certain steps of the pathway, such as incubating short rRNA mimics with AFs to promote RNA annealing or heteroduplex unwinding, RNA modification (e.g., methylation), or RNA processing (e.g., A_2 and A_3 cleavage). These assays revealed that AF Utp14 stimulates the RNA helicase Dhr1 (106), Esf2 stimulates the helicase Dbp8 (140), and Pfa1 stimulates the helicase Prp43 (141). Dhr1 unwound U3–18S duplexes in vitro (107), and ATP-bound Rok1 helicase stabilized Rrp5 binding to mature 40S subunits (142). Moreover, the low intrinsic activity of the Nug1 GTPase was stimulated by potassium ions (143), whereas the Lsg1 GTPase was activated by the export factor Nmd3 together with 60S subunits (82). Regarding RNA modification, 2′-O-methylation of artificial RNA was reconstituted with purified C/D box snoRNPs (144), and the methyltransferase Emg1 (Nep1) bound to a model RNA target substrate (34). Last but not least, the putative PIN domain endonuclease Utp24 and also Rcl1, both of which are part of the 90S preribosome, cleaved in vitro at site A_2 using a short pre-rRNA element (104, 105). However, which of the two enzymes exerts the concerted A_1–A_2 cleavage in vivo remains an open question.

The information deduced from these restricted in vitro maturation assays could be significantly extended by using the appropriate native preribosomal particles as substrates incubated with different AFs. Examples include the following: (*a*) Rea1 AAA-ATPase-driven removal of the AFs Ytm1 and Rsa4 from nucleolar and nucleoplasmic pre-60S particles, respectively (75, 136); (*b*) in vitro release of Nug2 from pre-60S particles requiring its own GTPase activity plus the remodeling Rea1 ATPase (119); (*c*) Hrr25-kinase-driven stable incorporation of ribosomal uS3/Rps3 into pre-40S particles (76); (*d*) Drg1 AAA-ATPase-catalyzed removal of the ribosomal-like protein Rlp24 from pre-60S particles (138); and (*e*) Fun12/eIF5B-dependent cleavage of 20S > 18S rRNA occurring on pre-40S particles stimulated by mature 60S subunits (117).

Removal of the entire ITS2 from isolated pre-60S particles has been reproduced in vitro by a multitude of methods (145, 146). These assays recapitulated all the known steps of ITS2 processing (**Figure 5*a***), starting with cleavage at site C_2 within ITS2 by the endonuclease Las1. Next, processing of the resulting 26S pre-rRNA to 25S rRNA occurred, which required phosphorylation of the free 5′-OH group by the polynucleotide kinase Grc3 and subsequent 5′ > 3′ trimming by the exonuclease Rat1 and its cofactor Rai1 (29, 147, 148). The second C_2-cleavage-derived

pre-rRNA (7S) was trimmed to nearly mature 5.8S rRNA by adding the nuclear exosome, a conserved eukaryotic RNA processing complex containing multiple 3′ > 5′ exonucleases (28) and consisting of 13 recombinant subunits, and its cofactor, the helicase Mtr4 (146). Overall, these studies provided not only mechanistic insight into the ITS2 processing pathway, including the discovery that 26S pre-rRNA processing has to precede that of 7S pre-rRNA, but also structural clarification, as ITS2 processing is coupled with the dismantling of a transient hallmark structure—the foot (146) (**Figure 5*b***).

Notably, it was also possible to watch the nuclear exosome at work when it was docked to the pre-60S particle (149) (**Figure 5*c***). The transient exosome–pre-60S intermediate was biochemically trapped by incubating the pre-60S particle with an exosome carrying a mutant Rrp6 exonuclease and was structurally characterized by cryo-EM (149). Several exciting details were recognized in this supramolecular assembly, which together with previous findings enabled the following model to be deduced: Prior to 7S pre-rRNA processing, the ATP-dependent Mtr4 helicase is recruited to the pre-60S particle via the pre-60S adapter protein Nop53 (150). Next, the foot structure, consisting of the 7S rRNA and AFs Rlp7, Nsa3, and Nop15 (88, 126–128) (**Figure 5*b***), is remodeled by the Mtr4 helicase to make the 7S substrate RNA accessible for channeling into the exosome (146, 149). During or after these steps, the initial contact of Mtr4 to Nop53 is abandoned in favor of a tighter interaction of Mtr4 at several discrete sites of the pre-60S particle, which also brings the exosome closer to its pre-60S substrate to carry out its processing task (**Figure 5*c***). Besides seeing the docking in great detail, perhaps the most fascinating aspect is to watch how the 7S pre-rRNA substrate egresses from the pre-60S particle to the bottom of the exosome, where the catalytic subunit Rrp44 awaits the 3′ tip for nucleolytic trimming (**Figure 5*c***). Thus, in vitro reconstruction and structural characterization of ITS2 processing is a long-cherished dream come true in the field of exosome function and ribosome assembly.

IMPACT OF RIBOSOME BIOGENESIS FOR HEALTH AND DISEASE

The comprehensive structural and biochemical analyses of ribosome biogenesis intermediates have revealed a deep mechanistic insight into this process. Notably, a growing number of clinical studies have discovered that mutations within human orthologs of AFs or r-proteins are the cause of human diseases (151–153). Such dysfunctions, which are triggered by subtle mutations in ribosomal AFs or haploinsufficiency of r-proteins and which delay ribosome assembly or affect translation, are collectively termed ribosomopathies (**Supplemental Table 3**). Moreover, (partially) disturbed ribosome assembly activates the nucleolar stress response pathway, which is intimately linked to cancer development (154, 155). Due to the high conservation of ribosome biogenesis and function from yeast to man, the functional and structural progress described above will also stimulate a mechanistic understanding of these diseases and might contribute to the improvement of cancer treatments.

Supplemental Material >

Most inherited ribosomopathies are characterized by tissue-specific defects including erythropoiesis (causing anemia) or skeletal or craniofacial developmental alteration (151–153). Notably, many studies have revealed that defects in ribosome biogenesis activate the p53-dependent signal pathway, a process known as the nucleolar stress response or the impaired ribosome biogenesis checkpoint (156, 157). The key players of this signaling pathway are the transcription factor p53 and its antagonist, the ubiquitin ligase Mdm2, which marks p53 for degradation (**Supplemental Figure 2*a***). Thus, inhibition of the Mdm2–p53 interaction activates this signal cascade, which drives expression of antiproliferative and apoptotic genes. Several r-proteins have been found to interact with Mdm2, but they might be ineffective to disrupt the p53–Mmd2 interaction, as a

cellular excess of free r-proteins is rapidly degraded (reviewed in 154, 155). In contrast, the newly translated r-proteins uL18/Rpl5 and uL5/Rpl11 preassemble with an existing free pool of 5S rRNA to form the stable 5S RNP (158, 159) (**Supplemental Figure 2*b***). During defective ribosome biogenesis, the 5S RNP accumulates and binds via uL5 to Mdm2 (160) (**Supplemental Figure 2*c***), thereby triggering the activation of p53. Consistently, the completely assembled 5S RNP, but not its single components, is required to trigger the p53-dependent response (reviewed in 154, 155). Thus, active p53 alters the balance between proliferation, cell cycle arrest, and apoptosis, therefore causing anemia and developmental disorders. Accordingly, anemia and skeletal malformation in ribosomopathy mouse models can be suppressed by inactivation of p53 (161–163). Interestingly, the 5S RNP-dependent activation of p53 is caused not only by ribosome biogenesis stress but also by low nucleotide levels, nutrient starvation (reviewed in 154, 155), and possibly hypoxia or oxidative stress (**Supplemental Figure 2*a***), but it is independent from the DNA damage checkpoint (164, 165). Taken together, ribosome biogenesis is used as a major checkpoint in the signaling of various stress responses.

Supplemental Material >

Surprisingly, patients with ribosomopathies have a significantly increased risk of developing cancer, as diminished ribosome assembly and an upregulated p53 pathway would antagonize an increased proliferation rate. Thus, one could speculate that ribosomopathy patients exhibit a high evolutionary pressure to circumvent elevated p53 levels. Accordingly, spontaneous p53 inactivation might have a much stronger impact compared with that in a healthy organism. Consistently in this regard, a zebrafish model based on mutated r-proteins showed that tumors in these organisms do not express p53 (166). Moreover, the 5S RNP–Mdm2 pathway might also be a bona fide target for new approaches to cancer treatment (167–169). Many established chemotherapeutics affect ribosome biogenesis, resulting in a 5S RNP–Mdm2-dependent p53 activation (170, 171). However, more specific ribosome biogenesis inhibitors might be potent chemotherapeutics with reduced genotoxic activity (170), or they could be combined with classic chemotherapeutics. Along these lines, the Pestov laboratory used an AF mutant to induce the nucleolar stress response, which arrests healthy cells in the G1 phase. Such G1-arrested cells were protected against the cytotoxicity of the S-phase–specific topoisomerase I inhibitor and therefore allowed the specific elimination of p53-deficient cells (172). However, in therapeutic applications the nucleolar stress response has to be activated by inhibitors against polymerase I (167), for example, or inhibitors against AFs such as the AAA-ATPases Drg1 (173) or Rea1 (174) that block ribosome biogenesis in yeast. Future approaches have to clarify the specificity and toxicity of these compounds in mammalian cells and the efficiency of p53 activation.

CONCLUSIONS

Half a century of research has given us a reasonable perception of the eukaryotic ribosome assembly pathway. Now, we can begin to arrange the various structural snapshots of preribosomal particles to watch this dynamic pathway as if it were a movie in pseudoatomic resolution (**Figure 6**; **Supplemental Video 1**). However, for further mechanistic understanding, new in vitro maturation assays have to be developed. These assays ultimately will help to dissect the unresolved steps in a reductionist way. The outstanding questions are: How do the transitions occur between the already known preribosomal particles, and what triggers them? Particularly unclear are the 90S > pre-40S progression and the opening of the pre-60S pathway during coordinated pre-rRNA processing at sites A_1–A_2. Besides refining this in greater detail, it will be important to identify these various assembly intermediates in the cellular context. A first step toward this goal was the recent EM tomographic visualization of transcribing RNA polymerase I and assembly

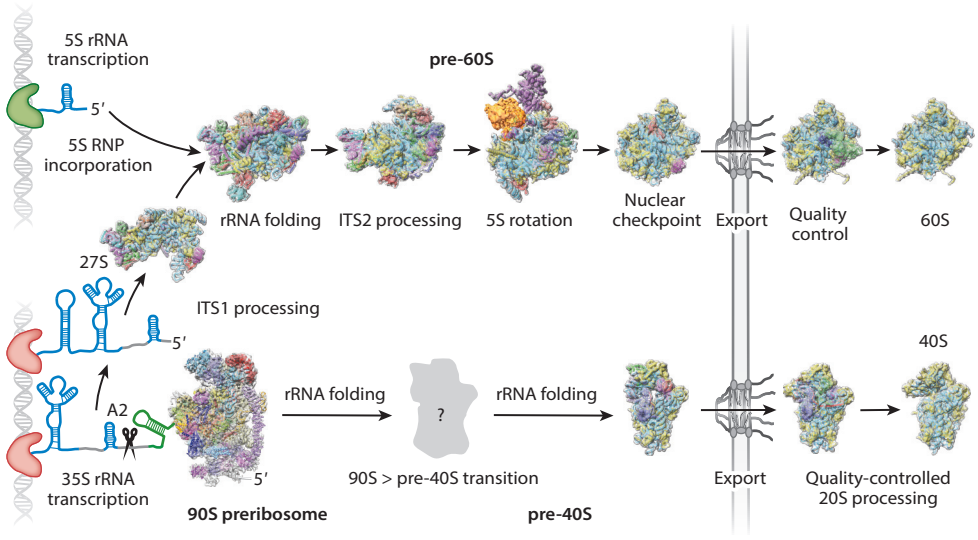

Figure 6

Structural snapshots of the eukaryotic ribosome assembly pathway. Cryo-EM structures of preribosomal particles are depicted according to their spatiotemporal assembly and maturation pathway, starting in the nucleolus during pre-rRNA transcription and ending in the cytoplasm, yielding mature 60S and 40S subunits. For detailed descriptions of these nascent ribosomal particles, see the main text. The rRNA is shown in tan and the r-proteins in yellow, whereas representative ribosome assembly factors are indicated in red, green, or blue. A list of high-resolution cryo-EM structures depicting these preribosomal particles is given in **Supplemental Tables 1 and 2**. Abbreviations: cryo-EM, cryo–electron microscopy; rRNA, ribosomal RNA.

Supplemental Material >

of the nascent rRNA into the earliest preribosomal particles (175). Super-resolution microscopy could be another means to verify the spatiotemporal course of events during ribosome maturation. Another key question in this field to be further experimentally addressed is how exactly ribosome assembly is coupled to other cellular pathways such as gene expression, cell proliferation, apoptosis, stress response, and cancer development. The answers will be precious information that not only will increase our scientific understanding of this essential cellular process but also might hold the key for developing better medical treatments for ribosomopathies or cancer.

DISCLOSURE STATEMENT

The authors are not aware of any affiliations, memberships, funding, or financial holdings that might be perceived as affecting the objectivity of this review.

ACKNOWLEDGMENTS

We thank Drs. N. Kellner, V. Mitterer, and C. Dietrich for comments on the manuscript. Our work is supported by grants from the German Research Council (HU363/15-1, HU363/12-1, and BA2316/2-1). We apologize to the authors of many exciting research articles that could not be cited here due to article length restrictions.

LITERATURE CITED

1. Ban N, Beckmann R, Cate JH, Dinman JD, Dragon F, et al. 2014. A new system for naming ribosomal proteins. *Curr. Opin. Struct. Biol.* 24:165–69
2. Melnikov S, Ben-Shem A, Garreau de Loubresse N, Jenner L, Yusupova G, Yusupov M. 2012. One core, two shells: bacterial and eukaryotic ribosomes. *Nat. Struct. Mol. Biol.* 19:560–67
3. Scherrer K, Latham H, Darnell JE. 1963. Demonstration of an unstable RNA and of a precursor to ribosomal RNA in HeLa cells. *PNAS* 49:240–48
4. Scherrer K, Darnell JE. 1962. Sedimentation characteristics of rapidly labelled RNA from HeLa cells. *Biochem. Biophys. Res. Commun.* 7:486–90
5. Tamaoki T. 1966. The particulate fraction containing 45 s RNA in L cell nuclei. *J. Mol. Biol.* 15:624–39
6. Warner JR, Soeiro R. 1967. Nascent ribosomes from HeLa cells. *PNAS* 58:1984–90
7. Trapman J, Retèl J, Planta RJ. 1975. Ribosomal precursor particles from yeast. *Exp. Cell Res.* 90:95–104
8. Miller OL, Beatty BR. 1969. Visualization of nucleolar genes. *Science* 164:955–57
9. Scheer U, Rose KM. 1984. Localization of RNA polymerase I in interphase cells and mitotic chromosomes by light and electron microscopic immunocytochemistry. *PNAS* 81:1431–35
10. Spector DL, Ochs RL, Busch H. 1984. Silver staining, immunofluorescence, and immunoelectron microscopic localization of nucleolar phosphoproteins B23 and C23. *Chromosoma* 90:139–48
11. Hügle B, Hazan R, Scheer U, Franke WW. 1985. Localization of ribosomal protein S1 in the granular component of the interphase nucleolus and its distribution during mitosis. *J. Cell Biol.* 100:873–86
12. Udem SA, Warner JR. 1973. The cytoplasmic maturation of a ribosomal precursor ribonucleic acid in yeast. *J. Biol. Chem.* 248:1412–16
13. Udem SA, Warner JR. 1972. Ribosomal RNA synthesis in *Saccharomyces cerevisiae*. *J. Mol. Biol.* 65:227–42
14. Warner JR. 1989. Synthesis of ribosomes in *Saccharomyces cerevisiae*. *Microbiol. Rev.* 53:256–71
15. Wool IG. 1979. The structure and function of eukaryotic ribosomes. *Annu. Rev. Biochem.* 48:719–54
16. Kressler D, Linder P, De La Cruz J. 1999. Protein trans-acting factors involved in ribosome biogenesis in *Saccharomyces cerevisiae*. *Mol. Cell. Biol.* 19:7897–912
17. Venema J, Tollervey D. 1999. Ribosome synthesis in *Saccharomyces cerevisiae*. *Annu. Rev. Genet.* 33:261–311
18. Watkins NJ, Bohnsack MT. 2012. The box C/D and H/ACA snoRNPs: key players in the modification, processing and the dynamic folding of ribosomal RNA. *Wiley Interdiscip. Rev. RNA* 3:397–414
19. Prestayko AW, Tonato M, Busch H. 1970. Low molecular weight RNA associated with 28 s nucleolar RNA. *J. Mol. Biol.* 47:505–15
20. Calvet JP, Pederson T. 1981. Base-pairing interactions between small nuclear RNAs and nuclear RNA precursors as revealed by psoralen cross-linking in vivo. *Cell* 26:363–70
21. Watkins NJ, Segault V, Charpentier B, Nottrott S, Fabrizio P, et al. 2000. A common core RNP structure shared between the small nucleoar box C/D RNPs and the spliceosomal U4 snRNP. *Cell* 103:457–66
22. Beltrame M, Tollervey D. 1992. Identification and functional analysis of two U3 binding sites on yeast pre-ribosomal RNA. *EMBO J.* 11:1531–42
23. Tyc K, Steitz JA. 1992. A new interaction between the mouse 5′ external transcribed spacer of pre-rRNA and U3 snRNA detected by psoralen crosslinking. *Nucleic Acids Res.* 20:5375–82
24. Henras AK, Soudet J, Gerus M, Lebaron S, Caizergues-Ferrer M, et al. 2008. The post-transcriptional steps of eukaryotic ribosome biogenesis. *Cell. Mol. Life Sci.* 65:2334–59
25. Bally M, Hughes J, Cesareni G. 1988. SnR30: a new, essential small nuclear RNA from *Saccharomyces cerevisiae*. *Nucleic Acids Res.* 16:5291–303
26. Jarmolowski A, Zagorski J, Li HV, Fournier MJ. 1990. Identification of essential elements in U14 RNA of *Saccharomyces cerevisiae*. *EMBO J.* 9:4503–9
27. Tollervey D, Kiss T. 1997. Function and synthesis of small nucleolar RNAs. *Curr. Opin. Cell Biol.* 9:337–42
28. Mitchell P, Petfalski E, Shevchenko A, Mann M, Tollervey D. 1997. The exosome: a conserved eukaryotic RNA processing complex containing multiple 3′→5′ exoribonucleases. *Cell* 91:457–66

29. Henry Y, Wood H, Morrissey JP, Petfalski E, Kearsey S, Tollervey D. 1994. The 5′ end of yeast 5.8S rRNA is generated by exonucleases from an upstream cleavage site. *EMBO J.* 13:2452–63
30. Filipowicz W, Kiss T. 1993. Structure and function of nucleolar snRNPs. *Mol. Biol. Rep.* 18:149–56
31. Balakin AG, Smith L, Fournier MJ. 1996. The RNA world of the nucleolus: two major families of small RNAs defined by different box elements with related functions. *Cell* 86:823–34
32. Sharma S, Yang J, Watzinger P, Kotter P, Entian KD. 2013. Yeast Nop2 and Rcm1 methylate C2870 and C2278 of the 25S rRNA, respectively. *Nucleic Acids Res.* 41:9062–76
33. Lafontaine D, Delcour J, Glasser AL, Desgres J, Vandenhaute J. 1994. The *DIM1* gene responsible for the conserved $m^6{}_2Am^6{}_2A$ dimethylation in the 3′-terminal loop of 18 S rRNA is essential in yeast. *J. Mol. Biol.* 241:492–97
34. Meyer B, Wurm JP, Kotter P, Leisegang MS, Schilling V, et al. 2011. The Bowen-Conradi syndrome protein Nep1 (Emg1) has a dual role in eukaryotic ribosome biogenesis, as an essential assembly factor and in the methylation of Psi1191 in yeast 18S rRNA. *Nucleic Acids Res.* 39:1526–37
35. Sharma S, Langhendries JL, Watzinger P, Kotter P, Entian KD, Lafontaine DL. 2015. Yeast Kre33 and human NAT10 are conserved 18S rRNA cytosine acetyltransferases that modify tRNAs assisted by the adaptor Tan1/THUMPD1. *Nucleic Acids Res.* 43:2242–58
36. Natchiar SK, Myasnikov AG, Kratzat H, Hazemann I, Klaholz BP. 2017. Visualization of chemical modifications in the human 80S ribosome structure. *Nature* 551:472–77
37. Rocak S, Linder P. 2004. DEAD-box proteins: the driving forces behind RNA metabolism. *Nat. Rev. Mol. Cell Biol.* 5:232–41
38. Hurt E, Hannus S, Schmelzl B, Lau D, Tollervey D, Simos G. 1999. A novel in vivo assay reveals inhibition of ribosomal nuclear export in Ran-cycle and nucleoporin mutants. *J. Cell Biol.* 144:389–401
39. Moy TI, Silver PA. 1999. Nuclear export of the small ribosomal subunit requires the Ran-GTPase cycle and certain nucleoporins. *Genes Dev.* 13:2118–33
40. Pillet B, Mitterer V, Kressler D, Pertschy B. 2017. Hold on to your friends: dedicated chaperones of ribosomal proteins. *BioEssays* 39:1–12
41. Pausch P, Singh U, Ahmed YL, Pillet B, Murat G, et al. 2015. Co-translational capturing of nascent ribosomal proteins by their dedicated chaperones. *Nat. Commun.* 6:7494
42. Gadal O, Strauss D, Kessl J, Trumpower B, Tollervey D, Hurt E. 2001. Nuclear export of 60S ribosomal subunits depends on Xpo1p and requires a NES-containing factor Nmd3p that associates with the large subunit protein Rpl10p. *Mol. Cell. Biol.* 21:3405–15
43. Thomas F, Kutay U. 2003. Biogenesis and nuclear export of ribosomal subunits in higher eukaryotes depend on the CRM1 export pathway. *J. Cell Sci.* 116:2409–19
44. Trotta CR, Lund E, Kahan L, Johnson AW, Dahlberg JE. 2003. Coordinated nuclear export of 60S ribosomal subunits and NMD3 in vertebrates. *EMBO J.* 22:2841–51
45. Ho JHN, Kallstrom G, Johnson AW. 2000. Nmd3p is a Crm1p-dependent adapter protein for nuclear export of the large ribosomal subunit. *J. Cell Biol.* 151:1057–66
46. Nerurkar P, Altvater M, Gerhardy S, Schutz S, Fischer U, et al. 2015. Eukaryotic ribosome assembly and nuclear export. *Int. Rev. Cell Mol. Biol.* 319:107–40
47. Merwin JR, Bogar LB, Poggi SB, Fitch RM, Johnson AW, Lycan DE. 2014. Genetic analysis of the ribosome biogenesis factor Ltv1 of *Saccharomyces cerevisiae*. *Genetics* 198:1071–85
48. Fischer U, Schauble N, Schutz S, Altvater M, Chang Y, et al. 2015. A non-canonical mechanism for Crm1-export cargo complex assembly. *eLife* 4:e05745
49. Zemp I, Wild T, O'Donohue MF, Wandrey F, Widmann B, et al. 2009. Distinct cytoplasmic maturation steps of 40S ribosomal subunit precursors require hRio2. *J. Cell Biol.* 185:1167–80
50. Baßler J, Grandi P, Gadal O, Leßmann T, Tollervey D, et al. 2001. Identification of a 60S pre-ribosomal particle that is closely linked to nuclear export. *Mol. Cell* 8:517–29
51. Harnpicharnchai P, Jakovljevic J, Horsey E, Miles T, Roman J, et al. 2001. Composition and functional characterization of yeast 66s ribosome assembly intermediates. *Mol. Cell* 8:505–15
52. Saveanu C, Bienvenu D, Namane A, Gleizes PE, Gas N, et al. 2001. Nog2p, a putative GTPase associated with pre-60S subunits and required for late 60S maturation steps. *EMBO J.* 20:6475–84

53. Fatica A, Cronshaw AD, Dlakić M, Tollervey D. 2002. Ssf1p prevents premature processing of an early pre-60S ribosomal particle. *Mol. Cell* 9:341–51
54. Tschochner H, Hurt E. 2003. Pre-ribosomes on the road from the nucleolus to the cytoplasm. *Trends Cell Biol*. 13:255–63
55. Dragon F, Gallagher JE, Compagnone-Post PA, Mitchell BM, Porwancher KA, et al. 2002. A large nucleolar U3 ribonucleoprotein required for 18S ribosomal RNA biogenesis. *Nature* 417:967–70
56. Grandi P, Rybin V, Baßler J, Petfalski E, Strauss D, et al. 2002. 90S pre-ribosomes include the 35S pre-rRNA, the U3 snoRNP, and 40S subunit processing factors but predominantly lack 60S synthesis factors. *Mol. Cell* 10:105–15
57. Milkereit P, Gadal O, Podtelejnikov A, Trumtel S, Gas N, et al. 2001. Maturation and intranuclear transport of pre-ribosomes requires Noc proteins. *Cell* 105:499–509
58. Perez-Fernandez J, Roman A, De Las Rivas J, Bustelo XR, Dosil M. 2007. The 90S preribosome is a multimodular structure that is assembled through a hierarchical mechanism. *Mol. Cell. Biol.* 27:5414–29
59. Granneman S, Gallagher JE, Vogelzangs J, Horstman W, van Venrooij WJ, et al. 2003. The human Imp3 and Imp4 proteins form a ternary complex with hMpp10, which only interacts with the U3 snoRNA in 60–80S ribonucleoprotein complexes. *Nucleic Acids Res*. 31:1877–87
60. Hierlmeier T, Merl J, Sauert M, Perez-Fernandez J, Schultz P, et al. 2013. Rrp5p, Noc1p and Noc2p form a protein module which is part of early large ribosomal subunit precursors in *S. cerevisiae*. *Nucleic Acids Res*. 41:1191–210
61. de la Cruz J, Karbstein K, Woolford JL Jr. 2015. Functions of ribosomal proteins in assembly of eukaryotic ribosomes in vivo. *Annu. Rev. Biochem.* 84:93–129
62. Ferreira-Cerca S, Poll G, Gleizes PE, Tschochner H, Milkereit P. 2005. Roles of eukaryotic ribosomal proteins in maturation and transport of pre-18S rRNA and ribosome function. *Mol. Cell* 20:263–75
63. Krogan NJ, Peng WT, Cagney G, Robinson MD, Haw R, et al. 2004. High-definition macromolecular composition of yeast RNA-processing complexes. *Mol. Cell* 13:225–39
64. McCann KL, Charette JM, Vincent NG, Baserga SJ. 2015. A protein interaction map of the LSU processome. *Genes Dev*. 29:862–75
65. Vincent NG, Charette JM, Baserga SJ. 2018. The SSU processome interactome in *Saccharomyces cerevisiae* reveals novel protein subcomplexes. *RNA* 24:77–89
66. Baßler J, Ahmed YL, Kallas M, Kornprobst M, Calvino FR, et al. 2017. Interaction network of the ribosome assembly machinery from a eukaryotic thermophile. *Protein Sci*. 26:327–42
67. Jakob S, Ohmayer U, Neueder A, Hierlmeier T, Perez-Fernandez J, et al. 2012. Interrelationships between yeast ribosomal protein assembly events and transient ribosome biogenesis factors interactions in early pre-ribosomes. *PLOS ONE* 7:e32552
68. Hunziker M, Barandun J, Petfalski E, Tan D, Delan-Forino C, et al. 2016. UtpA and UtpB chaperone nascent pre-ribosomal RNA and U3 snoRNA to initiate eukaryotic ribosome assembly. *Nat. Commun.* 7:12090
69. Zhang C, Sun Q, Chen R, Chen X, Lin J, Ye K. 2016. Integrative structural analysis of the UTPB complex, an early assembly factor for eukaryotic small ribosomal subunits. *Nucleic Acids Res*. 44:7475–86
70. Granneman S, Kudla G, Petfalski E, Tollervey D. 2009. Identification of protein binding sites on U3 snoRNA and pre-rRNA by UV cross-linking and high-throughput analysis of cDNAs. *PNAS* 106:9613–18
71. Zhang L, Wu C, Cai G, Chen S, Ye K. 2016. Stepwise and dynamic assembly of the earliest precursors of small ribosomal subunits in yeast. *Genes Dev*. 30:718–32
72. Chen W, Xie Z, Yang F, Ye K. 2017. Stepwise assembly of the earliest precursors of large ribosomal subunits in yeast. *Nucleic Acids Res*. 45:6837–47
73. Chaker-Margot M, Hunziker M, Barandun J, Dill BD, Klinge S. 2015. Stage-specific assembly events of the 6-MDa small-subunit processome initiate eukaryotic ribosome biogenesis. *Nat. Struct. Mol. Biol.* 22:920–23
74. Nissan TA, Galani K, Maco B, Tollervey D, Aebi U, Hurt E. 2004. A pre-ribosome with a tadpole-like structure functions in ATP-dependent maturation of 60S subunits. *Mol. Cell* 15:295–301

75. Ulbrich C, Diepholz M, Baßler J, Kressler D, Pertschy B, et al. 2009. Mechanochemical removal of ribosome biogenesis factors from nascent 60S ribosomal subunit. *Cell* 138:911–22
76. Schäfer T, Maco B, Petfalski E, Tollervey D, Bottcher B, et al. 2006. Hrr25-dependent phosphorylation state regulates organization of the pre-40S subunit. *Nature* 441:651–55
77. Strunk B, Loucks C, Su M, Vashisth H, Cheng S, et al. 2011. Ribosome assembly factors prevent premature translation initiation by 40S assembly intermediates. *Science* 333:1449–502
78. Bradatsch B, Leidig C, Granneman S, Gnadig M, Tollervey D, et al. 2012. Structure of the pre-60S ribosomal subunit with nuclear export factor Arx1 bound at the exit tunnel. *Nat. Struct. Mol. Biol.* 19:1234–41
79. Larburu N, Montellese C, O'Donohue MF, Kutay U, Gleizes PE, Plisson-Chastang C. 2016. Structure of a human pre-40S particle points to a role for RACK1 in the final steps of 18S rRNA processing. *Nucleic Acids Res.* 44:8465–78
80. Greber BJ, Boehringer D, Montellese C, Ban N. 2012. Cryo-EM structures of Arx1 and maturation factors Rei1 and Jjj1 bound to the 60S ribosomal subunit. *Nat. Struct. Mol. Biol.* 19:1228–33
81. Sengupta J, Bussiere C, Pallesen J, West M, Johnson AW, Frank J. 2010. Characterization of the nuclear export adaptor protein Nmd3 in association with the 60S ribosomal subunit. *J. Cell Biol.* 189:1079–86
82. Malyutin AG, Musalgaonkar S, Patchett S, Frank J, Johnson AW. 2017. Nmd3 is a structural mimic of eIF5A, and activates the cpGTPase Lsg1 during 60S ribosome biogenesis. *EMBO J.* 36:854–68
83. Ma C, Yan K, Tan D, Li N, Zhang Y, et al. 2016. Structural dynamics of the yeast Shwachman-Diamond syndrome protein (Sdo1) on the ribosome and its implication in the 60S subunit maturation. *Protein Cell* 7:187–200
84. Greber BJ, Gerhardy S, Leitner A, Leibundgut M, Salem M, et al. 2016. Insertion of the biogenesis factor Rei1 probes the ribosomal tunnel during 60S maturation. *Cell* 164:91–102
85. Kornprobst M, Turk M, Kellner N, Cheng J, Flemming D, et al. 2016. Architecture of the 90S preribosome: a structural view on the birth of the eukaryotic ribosome. *Cell* 166:380–93
86. Chaker-Margot M, Barandun J, Hunziker M, Klinge S. 2017. Architecture of the yeast small subunit processome. *Science* 355:aal1880
87. Johnson MC, Ghalei H, Doxtader KA, Karbstein K, Stroupe ME. 2017. Structural heterogeneity in pre-40S ribosomes. *Structure* 25:329–40
88. Wu S, Tutuncuoglu B, Yan K, Brown H, Zhang Y, et al. 2016. Diverse roles of assembly factors revealed by structures of late nuclear pre-60S ribosomes. *Nature* 534:133–37
89. Leidig C, Thoms M, Holdermann I, Bradatsch B, Berninghausen O, et al. 2014. 60S ribosome biogenesis requires rotation of the 5S ribonucleoprotein particle. *Nat. Commun.* 5:3491
90. Baßler J, Paternoga H, Holdermann I, Thoms M, Granneman S, et al. 2014. A network of assembly factors is involved in remodeling rRNA elements during preribosome maturation. *J. Cell Biol.* 207:481–98
91. Shu S, Ye K. 2018. Structural and functional analysis of ribosome assembly factor Efg1. *Nucleic Acids Res.* 46:2096–106
92. Kressler D, Hurt E, Baßler J. 2017. A puzzle of life: crafting ribosomal subunits. *Trends Biochem. Sci.* 42:640–54
93. Greber BJ. 2016. Mechanistic insight into eukaryotic 60S ribosomal subunit biogenesis by cryo-electron microscopy. *RNA* 22:1643–62
94. Barandun J, Hunziker M, Klinge S. 2018. Assembly and structure of the SSU processome—a nucleolar precursor of the small ribosomal subunit. *Curr. Opin. Struct. Biol.* 49:85–93
95. Biedka S, Wu S, LaPeruta AJ, Gao N, Woolford JL Jr. 2017. Insights into remodeling events during eukaryotic large ribosomal subunit assembly provided by high resolution cryo-EM structures. *RNA Biol.* 14:1306–13
96. Sun Q, Zhu X, Qi J, An W, Lan P, et al. 2017. Molecular architecture of the 90S small subunit preribosome. *eLife* 6:e22086
97. Cheng J, Kellner N, Berninghausen O, Hurt E, Beckmann R. 2017. 3.2-Å-resolution structure of the 90S preribosome before A1 pre-rRNA cleavage. *Nat. Struct. Mol. Biol.* 24:954–64
98. Barandun J, Chaker-Margot M, Hunziker M, Molloy KR, Chait BT, Klinge S. 2017. The complete structure of the small-subunit processome. *Nat. Struct. Mol. Biol.* 24:944–53

99. Rout MP, Field MC. 2017. The evolution of organellar coat complexes and organization of the eukaryotic cell. *Annu. Rev. Biochem.* 86:637–57
100. Fernandez-Pevida A, Kressler D, de la Cruz J. 2015. Processing of preribosomal RNA in *Saccharomyces cerevisiae*. *Wiley Interdiscip. Rev. RNA* 6:191–209
101. Phipps KR, Charette J, Baserga SJ. 2011. The small subunit processome in ribosome biogenesis—progress and prospects. *Wiley Interdiscip. Rev. RNA* 2:1–21
102. Tomecki R, Labno A, Drazkowska K, Cysewski D, Dziembowski A. 2015. hUTP24 is essential for processing of the human rRNA precursor at site A1, but not at site A0. *RNA Biol.* 12:1010–29
103. Bleichert F, Granneman S, Osheim YN, Beyer AL, Baserga SJ. 2006. The PINc domain protein Utp24, a putative nuclease, is required for the early cleavage steps in 18S rRNA maturation. *PNAS* 103:9464–69
104. Wells GR, Weichmann F, Colvin D, Sloan KE, Kudla G, et al. 2016. The PIN domain endonuclease Utp24 cleaves pre-ribosomal RNA at two coupled sites in yeast and humans. *Nucleic Acids Res.* 44:5399–409
105. Horn DM, Mason SL, Karbstein K. 2011. Rcl1 protein, a novel nuclease for 18 S ribosomal RNA production. *J. Biol. Chem.* 286:34082–87
106. Zhu J, Liu X, Anjos M, Correll CC, Johnson AW. 2016. Utp14 recruits and activates the RNA helicase Dhr1 to undock U3 snoRNA from the preribosome. *Mol. Cell. Biol.* 36:965–78
107. Sardana R, Liu X, Granneman S, Zhu J, Gill M, et al. 2015. The DEAH-box helicase Dhr1 dissociates U3 from the pre-rRNA to promote formation of the central pseudoknot. *PLOS Biol.* 13:e1002083
108. Scaiola A, Pena C, Weisser M, Bohringer D, Leibundgut M, et al. 2018. Structure of a eukaryotic cytoplasmic pre-40S ribosomal subunit. *EMBO J.* 37:e98499
109. Heuer A, Thomson E, Schmidt C, Berninghausen O, Becker T, et al. 2017. Cryo-EM structure of a late pre-40S ribosomal subunit from *Saccharomyces cerevisiae*. *eLife* 6:e30189
110. Ghalei H, Schaub FX, Doherty JR, Noguchi Y, Roush WR, et al. 2015. Hrr25/CK1δ-directed release of Ltv1 from pre-40S ribosomes is necessary for ribosome assembly and cell growth. *J. Cell Biol.* 208:745–59
111. Mitterer V, Gantenbein N, Birner-Gruenberger R, Murat G, Bergler H, et al. 2016. Nuclear import of dimerized ribosomal protein Rps3 in complex with its chaperone Yar1. *Sci. Rep.* 6:36714
112. Turowski TW, Lebaron S, Zhang E, Peil L, Dudnakova T, et al. 2014. Rio1 mediates ATP-dependent final maturation of 40S ribosomal subunits. *Nucleic Acids Res.* 42:12189–99
113. Strunk BS, Novak MN, Young CL, Karbstein K. 2012. A translation-like cycle is a quality control checkpoint for maturing 40S ribosome subunits. *Cell* 150:111–21
114. Ferreira-Cerca S, Kiburu I, Thomson E, LaRonde N, Hurt E. 2014. Dominant Rio1 kinase/ATPase catalytic mutant induces trapping of late pre-40S biogenesis factors in 80S-like ribosomes. *Nucleic Acids Res.* 42:8635–47
115. Belhabich-Baumas K, Joret C, Jady BE, Plisson-Chastang C, Shayan R, et al. 2017. The Rio1p ATPase hinders premature entry into translation of late pre-40S pre-ribosomal particles. *Nucleic Acids Res.* 45:10824–36
116. Ghalei H, Trepreau J, Collins JC, Bhaskaran H, Strunk BS, Karbstein K. 2017. The ATPase Fap7 tests the ability to carry out translocation-like conformational changes and releases Dim1 during 40S ribosome maturation. *Mol. Cell* 67:990–1000
117. Lebaron S, Schneider C, van Nues RW, Swiatkowska A, Walsh D, et al. 2012. Proofreading of pre-40S ribosome maturation by a translation initiation factor and 60S subunits. *Nat. Struct. Mol. Biol.* 19:744–53
118. Ameismeier M, Cheng J, Berninghausen O, Beckmann R. 2018. Visualizing late states of human 40S ribosomal subunit maturation. *Nature* 558:249–53
119. Matsuo Y, Granneman S, Thoms M, Manikas RG, Tollervey D, Hurt E. 2014. Coupled GTPase and remodelling ATPase activities form a checkpoint for ribosome export. *Nature* 505:112–16
120. Sarkar A, Thoms M, Barrio-Garcia C, Thomson E, Flemming D, et al. 2017. Preribosomes escaping from the nucleus are caught during translation by cytoplasmic quality control. *Nat. Struct. Mol. Biol.* 24:1107–15

121. Rodriguez-Galan O, Garcia-Gomez JJ, Kressler D, de la Cruz J. 2015. Immature large ribosomal subunits containing the 7S pre-rRNA can engage in translation in *Saccharomyces cerevisiae*. *RNA Biol*. 12:838–46
122. Biedka S, Micic J, Wilson D, Brown H, Diorio-Toth L, Woolford JL Jr. 2018. Hierarchical recruitment of ribosomal proteins and assembly factors remodels nucleolar pre-60S ribosomes. *J. Cell Biol.* 217:2503–18
123. Lebreton A, Rousselle JC, Lenormand P, Namane A, Jacquier A, et al. 2008. 60S ribosomal subunit assembly dynamics defined by semi-quantitative mass spectrometry of purified complexes. *Nucleic Acids Res*. 36:4988–99
124. Ma C, Wu S, Li N, Chen Y, Yan K, et al. 2017. Structural snapshot of cytoplasmic pre-60S ribosomal particles bound by Nmd3, Lsg1, Tif6 and Reh1. *Nat. Struct. Mol. Biol.* 24:214–20
125. Weis F, Giudice E, Churcher M, Jin L, Hilcenko C, et al. 2015. Mechanism of eIF6 release from the nascent 60S ribosomal subunit. *Nat. Struct. Mol. Biol.* 22:914–19
126. Kater L, Thoms M, Barrio-Garcia C, Cheng J, Ismail S, et al. 2017. Visualizing the assembly pathway of nucleolar pre-60S ribosomes. *Cell* 171:1599–610
127. Sanghai ZA, Miller L, Molloy KR, Barandun J, Hunziker M, et al. 2018. Modular assembly of the nucleolar pre-60S ribosomal subunit. *Nature* 556:126–29
128. Zhou D, Zhu X, Zheng S, Tan D, Dong MQ, Ye K. 2018. Cryo-EM structure of an early precursor of large ribosomal subunit reveals a half-assembled intermediate. *Protein Cell*. **https://doi.org/10.1007/s13238-018-0526-7**
129. van Nues RW, Rientjes JM, Morre SA, Mollee E, Planta RJ, et al. 1995. Evolutionarily conserved structural elements are critical for processing of Internal Transcribed Spacer 2 from *Saccharomyces cerevisiae* precursor ribosomal RNA. *J. Mol. Biol.* 250:24–36
130. van der Sande CA, Kwa M, van Nues RW, van Heerikhuizen H, Raue HA, Planta RJ. 1992. Functional analysis of internal transcribed spacer 2 of *Saccharomyces cerevisiae* ribosomal DNA. *J. Mol. Biol.* 223:899–910
131. Gadal O, Strauss D, Petfalski E, Gleizes PE, Gas N, et al. 2002. Rlp7p is associated with 60S preribosomes, restricted to the granular component of the nucleolus, and required for pre-rRNA processing. *J. Cell Biol.* 157:941–51
132. Adams CC, Jakovljevic J, Roman J, Harnpicharnchai P, Woolford JL Jr. 2002. *Saccharomyces cerevisiae* nucleolar protein Nop7p is necessary for biogenesis of 60S ribosomal subunits. *RNA* 8:150–65
133. Madru C, Lebaron S, Blaud M, Delbos L, Pipoli J, et al. 2015. Chaperoning 5S RNA assembly. *Genes Dev*. 29:1432–46
134. Asano N, Kato K, Nakamura A, Komoda K, Tanaka I, Yao M. 2015. Structural and functional analysis of the Rpf2–Rrs1 complex in ribosome biogenesis. *Nucleic Acids Res*. 43:4746–57
135. Kharde S, Calvino FR, Gumiero A, Wild K, Sinning I. 2015. The structure of Rpf2–Rrs1 explains its role in ribosome biogenesis. *Nucleic Acids Res*. 43:7083–95
136. Baßler J, Kallas M, Ulbrich C, Thoms M, Pertschy B, Hurt E. 2010. The AAA-ATPase Rea1 drives removal of biogenesis factors during multiple stages of 60S ribosome assembly. *Mol. Cell* 38:712–21
137. Hiraishi N, Ishida YI, Sudo H, Nagahama M. 2018. WDR74 participates in an early cleavage of the pre-rRNA processing pathway in cooperation with the nucleolar AAA-ATPase NVL2. *Biochem. Biophys. Res. Commun.* 495:116–23
138. Kappel L, Loibl M, Zisser G, Klein I, Fruhmann G, et al. 2012. Rlp24 activates the AAA-ATPase Drg1 to initiate cytoplasmic pre-60S maturation. *J. Cell Biol.* 199:771–82
139. Traub P, Nomura M. 1968. Structure and function of *E. coli* ribosomes, V. Reconstitution of functionally active 30S ribosomal particles from RNA and proteins. *PNAS* 59:777–84
140. Granneman S, Lin C, Champion EA, Nandineni MR, Zorca C, Baserga SJ. 2006. The nucleolar protein Esf2 interacts directly with the DExD/H box RNA helicase, Dbp8, to stimulate ATP hydrolysis. *Nucleic Acids Res*. 34:3189–99

141. Lebaron S, Papin C, Capeyrou R, Chen YL, Froment C, et al. 2009. The ATPase and helicase activities of Prp43p are stimulated by the G-patch protein Pfa1p during yeast ribosome biogenesis. *EMBO J.* 28:3808–19
142. Khoshnevis S, Askenasy I, Johnson MC, Dattolo MD, Young-Erdos CL, et al. 2016. The DEAD-box protein Rok1 orchestrates 40S and 60S ribosome assembly by promoting the release of Rrp5 from pre-40S ribosomes to allow for 60S maturation. *PLOS Biol.* 14:e1002480
143. Manikas RG, Thomson E, Thoms M, Hurt E. 2016. The K^+-dependent GTPase Nug1 is implicated in the association of the helicase Dbp10 to the immature peptidyl transferase centre during ribosome maturation. *Nucleic Acids Res.* 44:1800–12
144. Galardi S, Fatica A, Bachi A, Scaloni A, Presutti C, Bozzoni I. 2002. Purified box C/D snoRNPs are able to reproduce site-specific 2′-O-methylation of target RNA in vitro. *Mol. Cell. Biol.* 22:6663–68
145. Gasse L, Flemming D, Hurt E. 2015. Coordinated ribosomal ITS2 RNA processing by the Las1 complex integrating endonuclease, polynucleotide kinase, and exonuclease activities. *Mol. Cell* 60:808–15
146. Fromm L, Falk S, Flemming D, Schuller JM, Thoms M, et al. 2017. Reconstitution of the complete pathway of ITS2 processing at the pre-ribosome. *Nat. Commun.* 8:1787
147. Pillon MC, Sobhany M, Stanley RE. 2018. Characterization of the molecular crosstalk within the essential Grc3/Las1 pre-rRNA processing complex. *RNA* 24:721–38
148. Pillon MC, Sobhany M, Borgnia MJ, Williams JG, Stanley RE. 2017. Grc3 programs the essential endoribonuclease Las1 for specific RNA cleavage. *PNAS* 114:E5530–38
149. Schuller JM, Falk S, Fromm L, Hurt E, Conti E. 2018. Structure of the nuclear exosome captured on a maturing preribosome. *Science* 360:219–22
150. Thoms M, Thomson E, Baßler J, Gnadig M, Griesel S, Hurt E. 2015. The exosome is recruited to RNA substrates through specific adaptor proteins. *Cell* 162:1029–38
151. Narla A, Ebert BL. 2010. Ribosomopathies: human disorders of ribosome dysfunction. *Blood* 115:3196–205
152. Danilova N, Gazda HT. 2015. Ribosomopathies: how a common root can cause a tree of pathologies. *Dis. Models Mech.* 8:1013–26
153. Yelick PC, Trainor PA. 2015. Ribosomopathies: global process, tissue specific defects. *Rare Dis.* 3:e1025185
154. Pelava A, Schneider C, Watkins NJ. 2016. The importance of ribosome production, and the 5S RNP-MDM2 pathway, in health and disease. *Biochem. Soc. Trans.* 44:1086–90
155. Bursac S, Brdovcak MC, Donati G, Volarevic S. 2014. Activation of the tumor suppressor p53 upon impairment of ribosome biogenesis. *Biochim. Biophys. Acta* 1842:817–30
156. Holmberg Olausson K, Nister M, Lindstrom MS. 2012. p53-dependent and -independent nucleolar stress responses. *Cells* 1:774–98
157. Pelletier J, Thomas G, Volarevic S. 2018. Ribosome biogenesis in cancer: new players and therapeutic avenues. *Nat. Rev. Cancer* 18:51–63
158. Onofrillo C, Galbiati A, Montanaro L, Derenzini M. 2017. The pre-existing population of 5S rRNA effects p53 stabilization during ribosome biogenesis inhibition. *Oncotarget* 8:4257–67
159. Bursac S, Brdovcak MC, Pfannkuchen M, Orsolic I, Golomb L, et al. 2012. Mutual protection of ribosomal proteins L5 and L11 from degradation is essential for p53 activation upon ribosomal biogenesis stress. *PNAS* 109:20467–72
160. Zheng J, Lang Y, Zhang Q, Cui D, Sun H, et al. 2015. Structure of human MDM2 complexed with RPL11 reveals the molecular basis of p53 activation. *Genes Dev.* 29:1524–34
161. Jaako P, Debnath S, Olsson K, Zhang Y, Flygare J, et al. 2015. Disruption of the 5S RNP-Mdm2 interaction significantly improves the erythroid defect in a mouse model for Diamond-Blackfan anemia. *Leukemia* 29:2221–29
162. Barlow JL, Drynan LF, Hewett DR, Holmes LR, Lorenzo-Abalde S, et al. 2010. A p53-dependent mechanism underlies macrocytic anemia in a mouse model of human 5q- syndrome. *Nat. Med.* 16:59–66
163. Jones NC, Lynn ML, Gaudenz K, Sakai D, Aoto K, et al. 2008. Prevention of the neurocristopathy Treacher Collins syndrome through inhibition of p53 function. *Nat. Med.* 14:125–33

164. Macias E, Jin A, Deisenroth C, Bhat K, Mao H, et al. 2010. An ARF-independent c-MYC-activated tumor suppression pathway mediated by ribosomal protein-Mdm2 interaction. *Cancer Cell* 18:231–43
165. Kamio T, Gu BW, Olson TS, Zhang Y, Mason PJ, Bessler M. 2016. Mice with a mutation in the *Mdm2* gene that interferes with MDM2/ribosomal protein binding develop a defect in erythropoiesis. *PLOS ONE* 11:e0152263
166. MacInnes AW, Amsterdam A, Whittaker CA, Hopkins N, Lees JA. 2008. Loss of p53 synthesis in zebrafish tumors with ribosomal protein gene mutations. *PNAS* 105:10408–13
167. Brighenti E, Trere D, Derenzini M. 2015. Targeted cancer therapy with ribosome biogenesis inhibitors: a real possibility? *Oncotarget* 6:38617–27
168. Quin JE, Devlin JR, Cameron D, Hannan KM, Pearson RB, Hannan RD. 2014. Targeting the nucleolus for cancer intervention. *Biochim. Biophys. Acta* 1842:802–16
169. Derenzini E, Rossi A, Trere D. 2018. Treating hematological malignancies with drugs inhibiting ribosome biogenesis: when and why. *J. Hematol. Oncol.* 11:75
170. Burger K, Muhl B, Harasim T, Rohrmoser M, Malamoussi A, et al. 2010. Chemotherapeutic drugs inhibit ribosome biogenesis at various levels. *J. Biol. Chem.* 285:12416–25
171. Bruno PM, Liu Y, Park GY, Murai J, Koch CE, et al. 2017. A subset of platinum-containing chemotherapeutic agents kills cells by inducing ribosome biogenesis stress. *Nat. Med.* 23:461–71
172. Sapio RT, Nezdyur AN, Krevetski M, Anikin L, Manna VJ, et al. 2017. Inhibition of post-transcriptional steps in ribosome biogenesis confers cytoprotection against chemotherapeutic agents in a p53-dependent manner. *Sci. Rep.* 7:9041
173. Loibl M, Klein I, Prattes M, Schmidt C, Kappel L, et al. 2014. The drug diazaborine blocks ribosome biogenesis by inhibiting the AAA-ATPase Drg1. *J. Biol. Chem.* 289:3913–22
174. Kawashima SA, Chen Z, Aoi Y, Patgiri A, Kobayashi Y, et al. 2016. Potent, reversible, and specific chemical inhibitors of eukaryotic ribosome biogenesis. *Cell* 167:512–24
175. Neyer S, Kunz M, Geiss C, Hantsche M, Hodirnau VV, et al. 2016. Structure of RNA polymerase I transcribing ribosomal DNA genes. *Nature* 540:607–10